Asian Journal of Pharmaceutical Sciences 17 (2022) 299–332

Available online at www.sciencedirect.com

ScienceDirect

journal homepage: www.elsevier.com/locate/AJPS

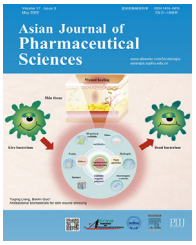

Review

Application of chitosan-based nanoparticles in skin wound healing

Hooi Leong Loo[a], *Bey Hing Goh*[b,c], *Learn-Han Lee*[d], *Lay Hong Chuah*[a,*]

[a] *School of Pharmacy, Monash University Malaysia, Selangor 47500, Malaysia*
[b] *Biofunctional Molecule Exploratory Research Group, School of Pharmacy, Monash University Malaysia, Selangor 47500, Malaysia*
[c] *College of Pharmaceutical Sciences, Zhejiang University, Hangzhou 310058, China*
[d] *Novel Bacteria and Drug Discovery (NBDD) Research Group, Microbiome and Bioresource Research Strength, Jeffrey Cheah School of Medicine and Health Sciences, Monash University Malaysia, Selangor 47500, Malaysia*

ARTICLE INFO

Article history:
Received 9 October 2021
Revised 31 March 2022
Accepted 1 April 2022

Keywords:
Biopolymer
Chitosan nanoparticle
Nanotechnology
Wound dressing
Wound healing

ABSTRACT

The rising prevalence of impaired wound healing and the consequential healthcare burdens have gained increased attention over recent years. This has prompted research into the development of novel wound dressings with augmented wound healing functions. Nanoparticle (NP)-based delivery systems have become attractive candidates in constructing such wound dressings due to their various favourable attributes. The non-toxicity, biocompatibility and bioactivity of chitosan (CS)-based NPs make them ideal candidates for wound applications. This review focusses on the application of CS-based NP systems for use in wound treatment. An overview of the wound healing process was presented, followed by discussion on the properties and suitability of CS and its NPs in wound healing. The wound healing mechanisms exerted by CS-based NPs were then critically analysed and discussed in sections, namely haemostasis, infection prevention, inflammatory response, oxidative stress, angiogenesis, collagen deposition, and wound closure time. The results of the studies were thoroughly reviewed, and contradicting findings were identified and discussed. Based on the literature, the gap in research and future prospects in this research area were identified and highlighted. Current evidence shows that CS-based NPs possess superior wound healing effects either used on their own, or as drug delivery vehicles to encapsulate wound healing agents. It is concluded that great opportunities and potentials exist surrounding the use of CSNPs in wound healing.

* Corresponding author.
E-mail address: alice.chuah@monash.edu (L.H. Chuah).
Peer review under responsibility of Shenyang Pharmaceutical University.

https://doi.org/10.1016/j.ajps.2022.04.001

1. Introduction

The prevalence of wounds in the global community is a rising concern. Data collected by numerous studies have brought light to a trend of increasing occurrence of wounds in tertiary care [1,2]. This has been highlighted by observational clinical studies conducted in several countries across the globe. In the United Kingdom, a cohort study reported a 71% increase of wound incidence from 2012 to 2018 within the National Health Service (NHS) [3]. Cases of chronic wounds increased from 0.94% in 2014 to 2.11% in 2018 in hospitals in Northern China, whereby the mean duration of hospitalization was 13 days [4]. Similarly, a 95.1% increase in wound episodes per 1000 patient admissions from 2013 to 2017 was reported by a case-control study conducted in Singapore [5]. The rising incidence of both acute and chronic wounds has imposed substantial burdens on healthcare. Data from the NHS shows that the estimated average costs per healed and unhealed wounds have increased by about 30.0% and 73.90% respectively from 2012 to 2018 [3].

Despite being a common presentation in the clinical setting, provision of optimal wound care remains a challenge to many physicians, especially in developing nations due to the limited resources available, coupled with the rising cost of wound care. In an effort to combat the significant difficulty in managing certain wound conditions and to alleviate the healthcare burden of treating wounds, development of novel wound treatment options warrants necessary attention [6]. Affordable wound treatments capable of improving wound healing outcomes are desirable and beneficial to both patients and the overall healthcare system [6]. Considering this notion, a great number of studies have explored numerous pharmaceutical formulations, utilising new technology and biomaterials with favourable properties to develop modern wound dressings [7–9].

This review aims to provide in depth discussion surrounding the use of chitosan (CS)-based nanoparticles (NPs) for the application in wound healing, which have been widely reported to have improved wound healing outcomes compared to CS alone and other forms of CS-based formulations. The small sizes of these CS-based NPs allow better permeation and distribution around the wound area [10]. We provide critical analysis on the various mechanisms on wound healing elicited by CS-based NPs, and their *in vitro* and *in vivo* effects. The main type of CS-based NP discussed in this review are CS NPs (CSNPs) which are polymeric NPs, either nanocapsules or nanospheres, formulated using CS. Other types of NPs such as nanogels, NP complexes, and polymeric micelles were also among some of the studies reviewed. The NPs were either used on their own or as a transport vehicle to deliver therapeutic agents such as antibiotics, natural compounds, and peptides. We include studies using different forms and derivatives of CS such as chitin, CS oligosaccharide (COS), and carboxymethyl CS (CMCS). Effects of CS-modified metal NPs were also highlighted in the context of wound healing. Discussion of the studies was categorised according to the wound healing mechanisms, namely haemostasis, antimicrobial effects, antioxidant effects, inflammatory response, angiogenesis, collagen deposition and wound closure rate acceleration. Research gap and future prospects in this research area were also addressed in this article.

2. The wound healing process

2.1. Skin physiology and wound healing

Representing the largest organ by surface area, the skin is the first line of defence separating the internal bodily environment from harmful external factors [11–13]. A breach in this defense and disruptions to the important functions of the skin may occur in the event of an injury [12]. Fortunately, regeneration of damaged skin tissue can be achieved to a certain extent through the process of wound healing [11]. Despite exhaustive efforts and extensive research in unraveling its physiological process, the complete mechanism surrounding wound healing still remains elusive [14]. Current evidence on the wound healing process can be categorised into chronological phases which overlap and are strongly dependent on each other [11].

2.2. Phases of wound healing

Haemostasis is the crucial first step in starting the wound healing process [11]. To prevent excessive blood loss, vasoconstriction of nearby vessels and aggregation of platelets take place to form a platelet plug in the initial stages almost immediately [11,14]. This is followed by the formation of thrombus via the coagulation cascade to temporarily seal any opening on the skin due to the wound [11].

The next chronological phase involves infiltration of immune cells, beginning with neutrophils and followed by macrophages to engulf any foreign invaders and debris present at the wound site [15,16]. The early inflammation phase involves the pro-inflammatory M1 macrophage phenotype, which releases cytokines such as interleukin (IL)−6 and IL-1β, as well as proteases known as matrix metalloproteinases (MMPs) [15]. During the late inflammation phase, anti-inflammatory M2 macrophages release several growth factors such as vascular endothelial growth factor (VEGF), insulin-like growth factor 1 (IGF-1) and transforming growth factor (TGF)-β along with anti-inflammatory cytokines such as IL-10 [11,15].

Subsequently, the proliferation phase kicks in, with the deposition of new granulation tissue, re-epithelialisation, and angiogenesis [12]. Fibroblast cells begin manufacturing new extracellular matrix (ECM) components such as collagen III, fibronectin, and hyaluronic acid [17,18]. Newly differentiated myofibroblasts also exert contractile forces to physically pull the edges of the wound together to facilitate wound contraction [17,18]. Meanwhile, a fresh epidermal layer begins to form on the surface of the wound through the proliferation and migration of keratinocytes during the process of re-epithelialisation [19]. Previously damaged or lost blood vessels are also slowly replaced during the process of angiogenesis [11,12].

Complete healing is characterised by a sealed opening, based on physical appearances on the external surface [11,20]. This is followed by the remodeling phase, which can last for several months or years after the wound has fully closed and involves the maturation of underlying skin tissue along with the manifestation of scars [11,20]. Changes which gradually occur during this phase include the replacement of type III collagen with type I collagen, along with the degradation of unnecessary ECM components by MMPs [11,21]. During this time, leaky new blood vessels undergo several changes to form more well-perfused vessels [11].

3. CS as a natural bioactive polymer

Mainly sourced from the exoskeletons of marine crustacean life, chitin is the second most abundantly occurring polysaccharide in nature [23]. However, its poor solubility in aqueous solutions limits its application [23]. Deacetylation of chitin results in the formation of CS, which comprises of D-glucosamine and N-acetyl D-glucosamine subunits linked together by $\beta-1,4$ glycosidic bonds [23]. Protonation of the amino groups along the CS polysaccharide chain makes it soluble under acidic conditions [23]. Studies have explored the benefits of CS in a wide range of applications across various research disciplines, including drug delivery vehicles, water treatment systems, and tissue engineering, to name a few [23,24].

Several features exhibited by CS and its derivatives have garnered attention from researchers to investigate its application in wound regeneration. Studies exploring the development of these materials have consistently shown accelerated wound healing rates and improved healing outcomes [25–28]. Its exceptional biocompatibility further substantiates its suitability for use in wound dressings [25].

4. CS and wound healing

4.1. *Wound healing properties of CS*

CS exerts its wound healing effect via several well-studied mechanisms. These include promotion of haemostasis, antimicrobial activity, free radical scavenging activity, and regulating the inflammatory response.

The physicochemical properties of CS and its polycationic nature allow it to promote haemostasis around the wound area through a few possible mechanisms identified by the current literature [29]. Positively charged CS is able to promote the aggregation of both negatively charged erythrocytes and platelets along with plasma proteins such as fibrinogen [29]. Collectively, these interactions help to facilitate blood aggregation and haemostasis.

To prevent unwanted infections at the wound site, CS exerts its antimicrobial effect via interactions between the polycationic polysaccharide chain with the negatively charged membrane components of bacterial cells [30,31]. Its ability to chelate trace amounts of metal ions on the surface membrane of bacterial cells also contributes to its antimicrobial properties to a smaller extent [30,31].

Over-production of reactive oxygen species (ROS) around the wound site can lead to direct damage in the form of lipid peroxidation and DNA modification to surrounding tissue; and indirect damage through the continuous promotion of pro-inflammatory cytokine release [32,33]. Having moderate scavenging activity against free radicals, CS is able to reduce ROS molecules by donating a hydrogen atom [34,35]. Both the hydroxyl groups and amino groups along the polymer chain contribute to this free radical scavenging effect [34,35]. However, the strong intermolecular and intramolecular hydrogen bonding within and among the CS polymer chains restrict the ability of these hydroxyl and amino groups from reacting with free radicals [34,35]. Hence, CS tends to exhibit mild anti-oxidative effects.

Any extension of inflammation beyond the healthy amount can disrupt the wound healing process and lead to chronic wounds [22,36]. CS with its immune stimulatory characteristics has been found to regulate both pro- and anti-inflammatory cytokines [37–39]. Inclination towards either pro- or anti-inflammatory activity of CS may be largely influenced by its physicochemical properties [40–42]. A small number of studies found and discussed that the inflammatory activity of CS may involve binding with CD14, TLR4, and CR3 receptors on macrophages [40–42]. Subsequent downstream effects involving production of tumor necrosis factor (TNF)-α, IL-6, nitric oxide, inducible nitric oxide synthase (iNOS) expression, nuclear factor kappa B (NF-κB) activation, and phosphorylation of mitogen-activated protein kinase (MAPK) signaling proteins are also found to be affected [40–42].

4.2. *Influence of polymer properties of CS on wound healing effects*

Being a natural polymer, variations in the molecular weight (MW) and degree of deacetylation (DDA) can have a significant influence on the wound healing properties of CS. The effects of these variations have been investigated in a number of studies.

4.2.1. *Molecular weight*

Generally, higher MW CS can be seen to be more favourable for haemostasis than lower MW CS to an extent [43,44]. It has been reported that CS oligomers with a MW of less than 8.6 kDa may not induce significant blood aggregation [43]. However, an increase in MW above 380 kDa was not found to produce notable changes in blood aggregation either [44]. Essentially, lower MW CS grant the benefit of larger surface area to volume ratios while higher MW CS provides greater amount of amine groups for interaction. A required balance between these two may be an explanation to the moderate range of MW producing optimal blood aggregation.

Under neutral pH conditions, lower MWs produce an overall improvement in antibacterial activity of CS [45]. Inversely, higher MWs have been correlated with an increase in antibacterial effects under acidic conditions [45]. These observations may possibly be due to the physical state of CS. The relatively small size of low MW CS may have more

interactions with bacteria cells due to a larger surface area to volume ratio. However, under acidic conditions, the larger positive charge of high MW CS may outweigh the benefits granted by the smaller sized low MW CS. Nevertheless, the antibacterial effects of CS based on its physicochemical properties tend to be difficult to predict due to various confounding factors. In fact, studies have reported varying results of the influence of MW on the antibacterial effects of CS [45–47].

In terms of free radical scavenging ability, studies have found a trend of lower MW CS leading to an increase in scavenging activity. Typically, as the MW of CS increases, the polymer chain lengthens [48–51]. This could possibly result in denser and more compact structures with an increase in intramolecular hydrogen bonding [48–51]. As a consequence, the ability of hydroxyl and amino groups present along the chain to reduce free radicals may be reduced [48–51].

Differences in immunological response have also been found between CS bearing different MWs. Although studies investigating this phenomenon are few in number, it has been found that low MW CS promote pro-inflammatory activity while high MW CS promote anti-inflammatory activity [40–42]. More studies will be required to describe these effects in greater detail.

4.2.2. *Degree of deacetylation*

Similar to the effects of MW, moderate DDA is found to produce better results in haemostasis [43,44,52]. Studies evaluating different DDA values have described either 68%, 64% – 72%, or 75% – 88% DDA produce the best haemostatic effects [43,44,52]. Striking a balance between the positive charges of CS with the negatively charged blood components is vital in producing optimal haemostatic effects [43].

Effects of DDA on the antibacterial properties of CS appear to be more straightforward than the effects of MW. Current literature generally reports a connection between increasing DDA with increasing antibacterial activity [46,53,54]. As DDA increases, the amount of amino groups available for ionisation increases. Consequently, the overall positive charge of CS increases, which enables stronger antibacterial effects.

A higher DDA may be correlated with higher free radical scavenging activity. Park et al. reported the highest scavenging effect when using hetero-CS with 90% DDA followed by 75% and 50% DDA [55]. These results were most prominent in 2,2-diphenyl-1-picrylhydrazyl (DPPH) radicals and not observed in hydroxyl radicals and superoxide radicals [55].

5. The use of NPs in wound management

NPs have emerged as a major developmental tool in diverse areas of medical and pharmaceutical research [56]. Their great potential owes largely to the incredibly small sizes, readily modifiable characteristics, as well as the ability to achieve controlled and targeted drug release [57]. In the development of wound dressings, NPs have been used either as a delivery vehicle or as a bioactive component on their own to achieve better wound healing outcomes (Fig. 2) [10,58,59].

As drug delivery vehicles, NPs are great carriers to transport active compounds to improve wound healing outcomes. They could also offer protection and prolong the half-lives of short-lived therapeutic agents, such as growth factors which are readily degraded by proteolytic enzymes; as well as nitric oxide which is generally transient in nature [58,59]. They have also been used to achieve effective and controlled delivery of antimicrobial agents and natural products for wound treatments [58,59]. Gene therapy which facilitates wound healing through modification of the wound microenvironment has also relied on nanoparticulate systems to deliver specific genetic material to the wound site [60].

Apart from serving as a delivery vehicle, some NPs have been explored extensively in promoting the wound healing process due to their intrinsic antibacterial properties [59]. Metallic NPs such as silver NPs (AgNPs), gold NPs (AuNPs), zinc oxide NPs (ZnONPs), copper NPs (CuNPs) and selenium NPs (SeNPs) have been widely studied for this purpose [59,61]. On the other hand, bioactive polymers such as alginate or CS and their derivatives represent another attractive source of building material for NP systems with exceptional wound healing effects [59,62,63].

6. CS-based NPs

6.1. *An introduction to CS-based NPs*

Scientific literature surrounding CS-based NPs is continuously growing at a rapid pace. In this review, CS-based NPs are defined as particles below 1000 nm in size synthesised using CS as the base material [64,65]. Numerous studies have been undertaken to identify the suitability of applying CS-based NPs in various biomedical fields such as wound healing and drug delivery [64–66].

CSNPs are the main type of CS-based NPs covered in this review article and comprise of polymeric NPs, either nanocapsules or nanospheres, synthesised using CS as the primary component [67]. Other types of NPs encountered while reviewing the literature include, CS-based nanogels, NP complexes, and polymeric micelles. Nanogels are nano-sized hydrogels which are composed of an interwoven network of cross-linked hydrophilic polymer chains such as CS [68]. NP complexes or nanoplexes have been defined as a drug-NP complex whereby an oppositely charged drug and polyelectrolyte interact to form a nanoplex [69]. A polymeric micelle is a self-assembled NP with a hydrophobic core and a hydrophilic shell prepared using amphiphilic polymers [70]. Other terms used in this review include carboxymethyl chitosan NPs (CMCSNPs) and chitin NPs (CNPs), which are polymeric NPs prepared using CMCS and chitin as the primary component, respectively. CS-modified metal NPs such as CS-modified AgNPs (CS-AgNPs), CS-modified AuNPs (CS-AuNPs), CS-modified SeNPs (CS-SeNPs), and CS-modified ZnONPs (CS-ZnONPs) will also be discussed in the following sections.

6.2. *Advantages of using CS-based NPs for wound healing*

Various formulations of CS are reported in the literature for wound healing, including but not limited to sponges and

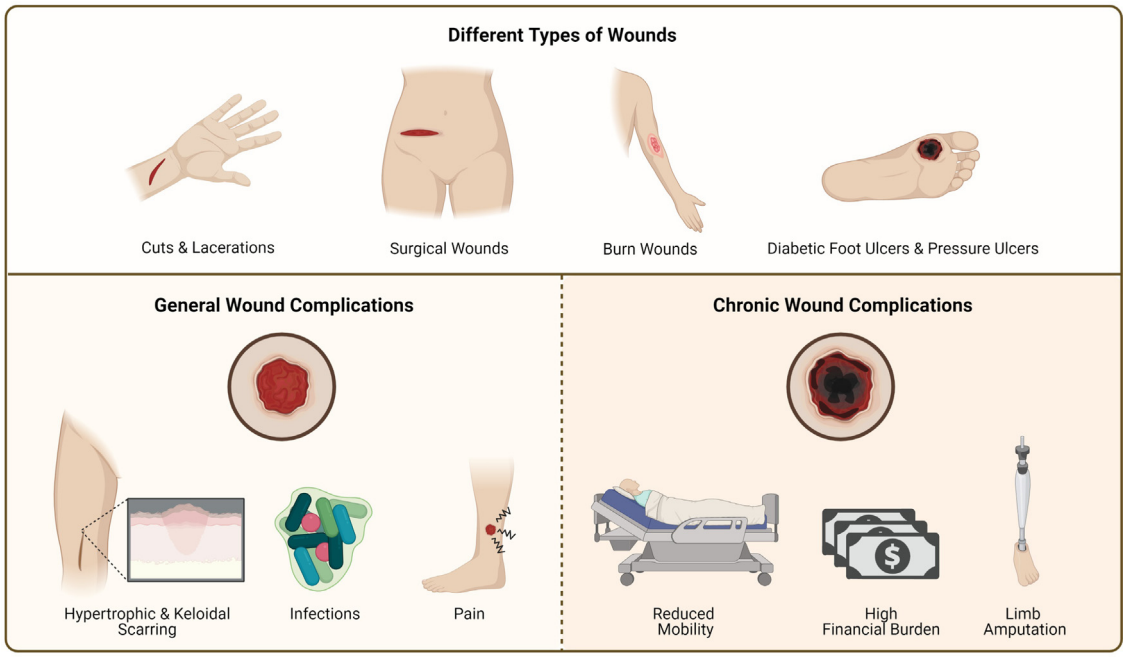

Fig. 1 – Illustration of the types of wounds and problems associated with wounds.

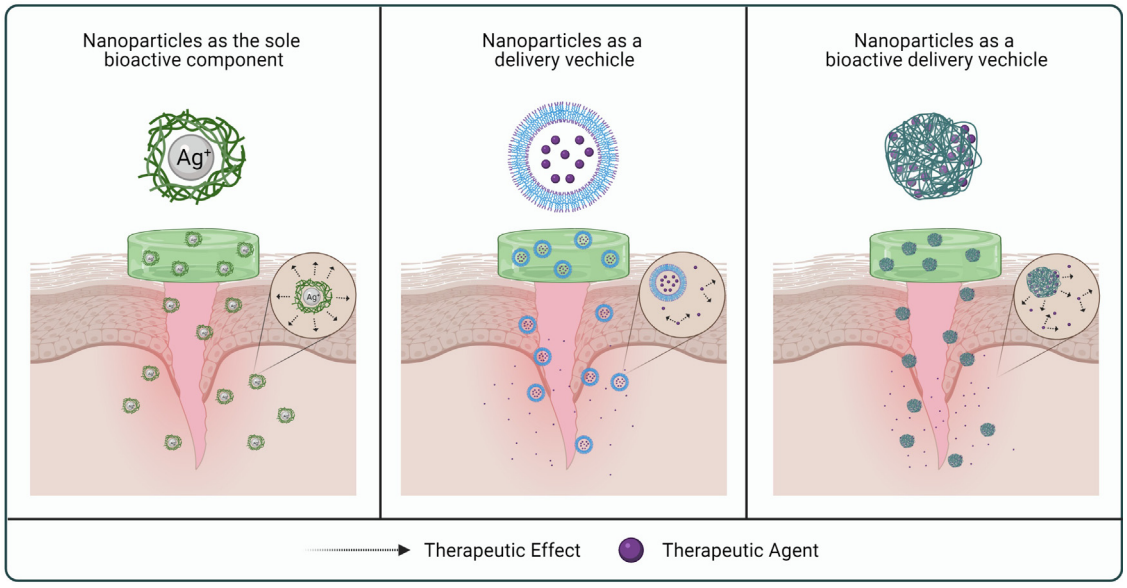

Fig. 2 – Illustration of the use of NPs in wound healing.

films which are made from CS as the base material. The effects of these relatively larger structures are not comparable to that of CS-based NPs, with their distinctive advantage of having significantly smaller particle sizes [71]. The nano-sized particles allow for improved penetration across skin tissue and possibly into the wound area for more efficient wound healing effects [71]. Additionally, the positive charge of polymeric CS-based NPs offers a unique range of benefits. As most CS-based NPs carry a strong positive charge due to the nature of the polymer, most CS-based NP formulations have good stability due the repulsion of like charges to prevent aggregation [72]. Strong positive charges on the surface of CS-based NPs also allow them to interact more readily with many negatively charged components such as cell surfaces, mucosal surfaces, and bacteria cells [72,73].

Having intrinsic wound healing properties, CS-based NPs can be used on their own, or as a vehicle to deliver therapeutic compounds to the wound. This further opens up more

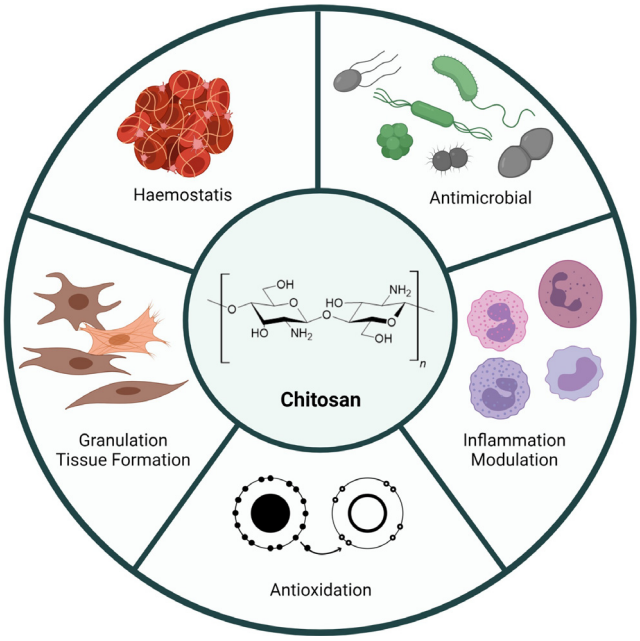

Fig. 3 – Summary of the wound healing properties exerted by CS.

opportunities for enhancing wound healing effects, which can be achieved by engineering the CS-based NPs to prolong the half-life of a specific compound, achieve a controlled-release effect, and enable targeted delivery of therapeutic compounds [10,65]. Therapeutic compounds with low stability can also be protected by the NPs in the drug delivery process for improved efficacy [10,57,74]. Problems associated with poor solubility of certain compounds can also be overcome by embedding them within CS-based NPs to be delivered efficiently [10,57,74]. By virtue of these two advantages, compounds which are not able to be ordinarily used therapeutically can now be feasible. The high surface to volume ratio also means that there is significantly more surface available for interaction to trigger the wound healing mechanism [75]. This enhanced feature could also be further exploited to distribute high amounts of active wound healing compounds more efficiently around the wound site [10,65]. Therapeutic compounds delivered using CS-based NPs have been shown to possess the added advantage of enhanced skin penetration and deposition [76–78]. Furthermore, compounds which exhibit toxicity at high concentrations may also show reduced cell toxicity by encapsulating them within CS-based NPs [79]. This shows that the safety of therapeutic compounds could also be improved through the formulation of CS-based NPs.

6.3. *Preparation methods of CSNPs, nanogels, NP complexes, and polymeric micelles*

Various methods in formulating different types of CS-based NPs have been studied extensively over the years. Different methods used in the preparation of CSNPs, CS-based nanogels, CS-based NP complexes, and CS-based polymeric micelles are discussed below.

6.3.1. *CSNPs*

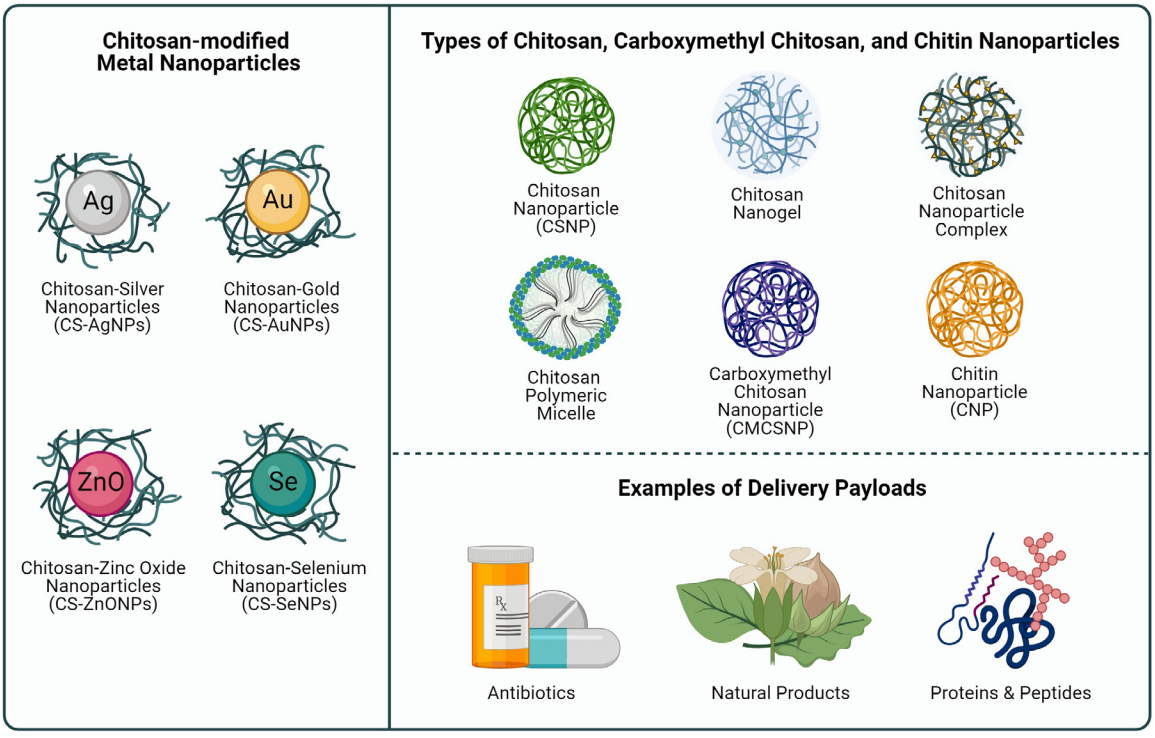

Fig. 4 – Illustration of the types of CS-based NPs, CMCSNPs, CNPs, and CS-modified NPs included in this literature review.

6.3.1.1. Ionic gelation Since the discovery of CSNPs, multiple preparation methods have been tested and evaluated to efficiently synthesize these NPs under different conditions. The most commonly reported method is the ionic gelation or ionotropic gelation method. This method takes advantage of the polycationic nature of CS where an oppositely charged ionic cross-linker, usually sodium tripolyphosphate (TPP), is added to induce the formation of NPs via electrostatic interactions [80]. CS is usually initially dissolved in an acetic acid, prior to the addition of TPP or other cross-linkers in this method [80]. The simplicity and efficiency of this method make it highly popular as it can be easily performed, and the NP properties can also be readily manipulated by adjusting the ratio of CS to the cross-linker added [80]. This method does not require the use of organic solvents.

6.3.1.2. Polyelectrolyte complex method The polyelectrolyte complex method is also fairly simple, where electrostatic interactions between a polycation such as CS take place with an anionic molecule to form polyelectrolyte complexes. Examples of common polyelectrolyte complexes are NPs formed by the spontaneous self-assembly of polycationic CS with alginate, chondroitin sulfate, hyaluronate, dextran sulfate, and carboxymethyl cellulose [81–83]. In some instances, anionic molecules intended to be incorporated into the NP can interact with CS to form these polyelectrolyte complexes [84,85].

6.3.1.3. Microemulsion method As opposed to the ionic gelation and polyelectrolyte complex methods, the microemulsion method requires the use of organic solvent. CS is initially prepared in an acidic aqueous solution, usually low concentration acetic acid, along with a cross-linker such as glutaraldehyde [86–88]. The solution is then added into a mixture of an organic solvent such as hexane containing a surfactant [86–88]. Cross-linking and the formation of CSNPs will then ensue while the mixture is allowed to stir for a duration of time [86–88]. Removal of the organic solvent can then be done by evaporation under low pressure [86–88]. Addition of calcium chloride and centrifugation also assists in the removal of excess surfactant via precipitation [86–88]. Purification of the NPs through processes such as dialysis followed by lyophilisation can then be done to obtain the final product.

6.3.1.4. Coprecipitation method By taking advantage of the solubility of CS at different pH values, the coprecipitation method is rather simple and can be easily performed. This method begins with dissolving CS in a low pH acidic solution such as acetic acid. The dissolved CS is then slowly added dropwise to an alkaline solution of pH 8.5 – 9.0 under continuous stirring which advertently causes its precipitation [89]. NPs can then be separated via centrifugation and reconstituted in an aqueous solution for further analysis [89]. This method has also been found to be applicable for both CS and lactic acid-grafted-CS copolymers along with the preparation of CS-coated magnetic NPs [89–92].

6.3.1.5. Emulsification solvent diffusion method The emulsification solvent diffusion method requires a large amount of shear force typically provided by high pressure homogenisation to synthesize CSNPs. In this method, aqueous CS solution is carefully added to a mixture of an organic solvent with a stabiliser to produce an emulsion [93–95]. The resulting mixture is then subjected to high pressure homogenisation to form NPs [93–95]. After applying high pressure homogenisation, the NPs can be separated by centrifugation or other means [93–95]. Addition of cross-linkers such as glutaraldehyde or ionic cross-linkers such as poly-γ-glutamic acid (γ-PGA) have been used by some studies in combination with this method to further facilitate NP formation [94,95].

6.3.2. CS-based nanogels

6.3.2.1. Physical gelation CS-based nanogels can be synthesised through the gelation of CS polymers under certain conditions. The physical gelation of CS to form nanogels through reverse emulsion can be achieved by mixing CS solutions within an emulsion containing a surfactant, followed by the addition of a base, such as ammonia to increase the pH to 9.0 [96]. This ensures the precipitation of the nanogels due to the poor solubility of CS under alkaline conditions [96].

6.3.2.2. Ionic gelation Similar to CS-based NPs, nanogels can also be synthesised through the ionic gelation of CS using a suitable cross-linker [97,98]. TPP again represents the most commonly used cross-linker for the synthesis of CSNPs as well as CS-based nanogels [97,98]. In this case, the gelation of CS occurs via ionic cross-linking to form a three-dimensional polymer network to form nanogels.

6.3.2.3. Inverse microemulsion Inverse microemulsion is a method whereby two microemulsions are prepared separately, one containing CS and another containing the cross-linker such as genipin or poly(ethyleneglycol bis(carboxymethyl)ether), $PEGB(COOH)_2$ [99,100]. The two microemulsions are then mixed together while stirring to allow nanogels to form via cross-linking [99,100]. After the nanogels have formed, they can then be separated through precipitation with ethanol [99,100].

6.3.3. CS-based NP complexes

Electrostatic interactions between negatively charged drug molecules with positively charged polycationic CS have been seen to produce NP complexes or nanoplexes via electrostatic interactions. Nguyen et al. described the preparation of ionised curcumin (CUR^{3-}) which was mixed with a solution of CS with stirring to form curcumin (CUR)-CS NP complexes [101]. By using this method, changes to the NP properties could be easily adjusted by manipulating the concentration of CUR^{3-}, pH of the solution, and CS: CUR^{3-} ratio [101]. The NP complex was also able to be formed with CUR^{3-} and COS [102].

6.3.4. CS-based polymeric micelles

CS exists as a hydrophilic polymer which does not self-assemble under normal conditions. To form an amphiphilic copolymer, hydrophobic modification of CS can be achieved by grafting hydrophobic molecules onto the polysaccharide

chain of CS [103]. The hydrophobic components can be fatty acids, cholesterol, other polymers, along with many others [103]. After modifying CS with the hydrophobic component, the new amphiphilic molecule will be able to self-assemble upon reaching a critical concentration in an aqueous solution [103]. If an organic solvent is required to dissolve certain components in the formulation, other methods of self-assembly can be employed, such as co-solvent evaporation, thin film hydration, and dialysis, to facilitate the removal of the solvent during or after the process [104,105].

7. Wound healing studies using CS-based NPs and CS-modified metal NPs

7.1. *Haemostasis*

7.1.1. *CSNPs*

Inadequacies in the haemostasis process can lead to catastrophic outcomes due to the inability to prevent excessive blood loss [106]. In a study using a thrombin generation assay, blood treated with CSNPs displayed two times higher thrombin levels than control, recording levels of 250 ng/ml and 120 ng/ml respectively [107]. This observation was explained through the polycationic nature of the CSNPs, which allows them to interact with negatively charged erythrocytes, causing quicker aggregation rates [107]. Additionally, the large surface area presented by the CSNPs provides a suitable site for platelet adhesion as well as adsorption of fibrinogen and plasma proteins, which assists in accelerating the haemostasis process [107]. Two studies have both demonstrated haemagglutination occurring in erythrocytes treated with blank CSNPs formed via ionic gelation with TPP [108,109]. Neutralistion of the samples with NaOH was found to improve the haemagglutination effect of CSNPs in one of the two studies [109]. Gopalakrishnan et al. had also found blank CSNPs to exhibit similar reductions in blood clotting time as ellagic acid when used at higher concentrations [108]. When combined as ellagic acid-loaded CSNPs, the effect on blood clotting time was found to be considerably enhanced [108]. Based on the proposed mechanism, CSNPs have an advantage over CS in promoting haemostasis as the smaller sizes of CSNPs grant them a greater surface area to volume ratio which enables better haemagglutination, platelet aggregation, and plasma protein adsorption. Under the same reasoning, smaller particle sizes and higher surface charges which lead to larger total surface area to volume ratios and attraction of negatively charged erythrocytes would improve haemostatic effects.

7.1.2. *CS-modified metal NPs*

A separate study had examined the effects of thiol-modified CS (TMC)-immobilised AgNP-loaded dressings on wound haemostasis *in vivo* [110]. This study used two separate animal models involving a liver injury model in mice and a rabbit ear model simulating venous rupture [110]. In both models, TMC and TMC-immobilised AgNP treatment groups showed similar blood clotting ability, achieving haemostasis in the shortest time, followed by the CS only group. All CS-based treatment groups had superior haemostatic activities compared to commercial poly(vinyl alcohol) dimethyl-formal (PVF) sponge and medical cotton group [110]. TMC and TMC-immobilised AgNP-loaded dressings were also found to produce a significantly lower amount of blood loss as compared to CS-based dressing alone, commercial PVF sponge, and medical cotton [110]. The authors proposed that the observed enhancement in haemostatic activity by TMC in contrast to CS could be due to the thiol group, which could potentially promote the activation of tissue factor, an important initiator of the coagulation cascade [110]. However, further investigation is needed to validate this notion.

7.2. *Antimicrobial properties*

7.2.1. *CSNPs*

The antibacterial mode of action of CS has been previously elaborated in the earlier section of this review. Antibacterial effects of polycationic CS are proposed to typically revolve around its interaction with negatively charged cell surfaces and chelation of metals. Interestingly, shorter-chained low MW CS and CSNPs have shown additional antimicrobial effects compared to larger-sized CS structures, in which the latter typically only involve interactions with bacterial cell surfaces [30,31,73,111]. The small sizes of CSNPs allow them to act locally on bacterial cell membranes and permeate across the bacterial cell wall to interfere with intracellular processes such as DNA transcription and mRNA synthesis [30,31,73,111].

A few studies have investigated the use of unloaded CSNPs for the purpose of wound healing in terms of their antimicrobial effects (Table 1 & Table 2). Wang et al. reported a statistically significant difference in antibacterial activity between CSNP-loaded calcium alginate hydrogels and CS-calcium alginate hydrogels [75]. At a concentration of 100 µg/ml CS in both groups, the CSNP-loaded calcium alginate hydrogel had more than twice the antibacterial activity against E. coli, and about three times the antibacterial activity against S. aureus as compared to the CS-calcium alginate hydrogel [75]. Overall, the calcium alginate hydrogel in combination with CSNPs produced a notably better antibacterial effect than the calcium alginate hydrogel formulated with unmodified CS [75]. This further supports the idea that CSNPs produce enhanced antibacterial activity than CS alone. Sami et al. had similarly demonstrated that CSNPs had higher antibacterial activity against S. aureus than E. coli [75,112]. Both of these studies had CSNPs with similar surface charges of +24.2 mV and greater than +30 mV, respectively [75,112]. The positive surface charge of the CSNPs in these two studies are reflective of the cationic nature of CS, which can be seen as a significant contributor to its antibacterial effects.

Concentration-dependent reductions in bacterial growth was reported in a study evaluating CSNP loaded in polyurethane membranes [113]. However, the increase in antibacterial activity due to increasing CSNP concentration was only observed against the Gram-positive S. aureus, while the activity against the Gram-negative P. aeruginosa remained constant regardless of CSNP concentration [113]. Despite this fact, the developed CSNPs in this study clearly exhibited greater antibacterial activity against P. aeruginosa than S. aureus, with differences between percentage reduction ranging from approximately 20% to 40% across all samples

Table 1 – Summary of wound healing studies evaluating the antimicrobial properties of CS-based NPs, CMCSNPs, and CS-modified metal NPs *in vitro*.

NP formulation	Active ingredient	Encapsulation efficiency	Size	Surface charge	Microbe	Key findings	Ref.
Blank CS-based NPs							
CSNP[a]	–	–	141.20 nm[†]	–	S. aureus, P. aeruginosa	• Dose-dependent antibacterial activity was observed against S. aureus. • Consistent antibacterial activity was observed for all concentrations of CSNPs against P. aeruginosa (63% – 69%).	[113]
CSNP[a]	–	–	77 nm[†]	> +30.00 mV	S. aureus, E. coli	• CSNPs displayed dose-dependent bacterial inhibition. • Higher inhibitory effects were observed against S. aureus (<50% survival) compared to E. coli (>50% survival).	[112]
CSNP[a]	–	–	208.40 ± 15.70 nm[†]	+24.20 ± 3.90 mV	S. aureus, E. coli	• CSNP-loaded calcium alginate hydrogels exhibited a dose-dependent antibacterial effect with greater effects against S. aureus than E. coli. • CSNP-loaded calcium alginate hydrogels had significantly higher antibacterial activity than CS-calcium alginate hydrogels.	[75]
Therapeutic compound loaded CS-based NPs							
Lecithin-coated CSNP[a]	Tigecycline (TGC)	22%	235 ± 20 nm[†]	+19 ± 5 mV	S. aureus	• TGC-loaded CSNPs had significantly lower minimum inhibitory concentration (MIC) values than TGC-loaded lecithin-coated CSNPs. • Unloaded CSNPs had consistently lower MIC values than unloaded lecithin-coated CSNPs. • The MIC values for unloaded CSNPs, TGC-loaded CSNPs, lecithin-coated CSNPs, and TGC-loaded lecithin-coated CSNPs were 0.3, 0.1, 1.2, and 0.4 mg, respectively.	[125]
CSNP[b]	SSD	89.71% ± 11.01%	51.67 ± 12.55 nm[†]	–	S. aureus, P. aeruginosa, E. coli, B. subtilis, C. albicans	• SSD-loaded CSNPs showed higher antibacterial activity against Gram-positive bacteria than Gram-negative bacteria. • Antifungal activity of SSD-loaded CSNPs ranged from 20.35% – 36.85% reduction rates.	[126]
CSNP[a]	Cefazolin (CEZ)	94.80% ± 0.47%	227.40 nm[†]	+48.80 mV	S. aureus	• Sodium alginate and pectin films containing the CEZ-loaded CSNPs achieved 100% inhibition at 24 h incubation.	[127]
CSNP[a]	CUR	99.93% ± 3.43%	279.70 ± 20.30 nm[†]	+52.40 ± 1.50 mV	S. aureus, P. aeruginosa	• Similar inhibitory activity was observed for both S. aureus and P. aeruginosa for all treatment groups. • CUR-loaded CSNPs had significantly higher inhibitory activity than blank CSNPs. • At 1000 µg, CUR-loaded CSNPs had a ZOI of ~25 mm while the positive control, gentamicin had a ZOI of 25 – 30 mm for both S. aureus and P. aeruginosa	[128]
Gelatin/CSNP[c]	EGCG	45.80% ± 3.70%	236.60 ± 7.80 nm[†]	+28.90 ± 1.20 mV	S. aureus, P. aeruginosa, E. coli	• EGCG-loaded gelatin/CSNPs with gentamicin had significantly larger ZOI than commercial Aquacel® Ag^+ dressings. • Largest ZOI was observed in P. aeruginosa followed by S. aureus, and E.coli.	[129]

(*continued on next page*)

Table 1 (*continued*)

NP formulation	Active ingredient	Encapsulation efficiency	Size	Surface charge	Microbe	Key findings	Ref.
CSNP[a]	H. pineodora	27.56%	158.70 nm[†]	+24.10 mV	S. aureus, MRSA, P. aeruginosa, E. coli, B. subtilis, B. cereus, P. mirabilis, S. typhimurium, Yersinia sp., K. pneumoniae, S. boydii, A. anitratus, C. albicans, C. utilis	• H. pineodora encapsulated in CSNPs had significantly larger ZOI than H. pineodora essential oil, CSNPs and chloramphenicol across all microorganisms tested except for C. albicans. • H. pineodora encapsulated in CSNPs showed 90.0% – 99.9% synergism between the H. pineodora and CSNP. • Up to 83.03% and 80.71% reduction in colony counts were observed in an *in vitro* collagen wound model and simulated wound fluid, respectively.	[119]
CSNP[a]	Insulin	77%	294.50 ± 21.92 nm[†]	+17.89 ± 0.74 mV	–	• Samples treated with wound dressings containing insulin-loaded CSNPs had lower microbial penetration across the wound dressing. • Optical density of the Brain heart infusion broth of the positive control (absorbance≈30) was significantly higher than dressings containing insulin-loaded CSNPs (absorbance<5), by Day 7.	[130]
CMCSNPs							
CMCSNP[d]	OH30	82.46 ± 1.11%	258.70 ± 13.30 nm[†]	+30.20 ± 5.10 mV	E. coli	• OH30-loaded CMCSNPs sustained 100% antibacterial activity while the unloaded CMCSNPs peaked at less than 50%.	[120]
CMCSNP[e]	OH30	92.14 ± 1.05%	164.60 ± 5.00 nm[†]	−37.60 ± 1.50 mV	S. aureus, E. coli	• Dressings containing OH30-loaded CMCSNP produced >80% antibacterial activity against both S. aureus and E. coli. • Unloaded dressings produced around 40% and 20% antibacterial activity against S. aureus and E. coli, respectively.	[121]
CS-modified metal NPs							
CS-ZnONP[‖]	ZnO	–	~180 nm[¶]	–	S. aureus, E. coli, M. luteus	• Nanocomposites loaded with CS-ZnONPs had higher antimicrobial activity on Gram-positive bacteria than Gram-negative bacteria. • At 7.5 wt% concentration, CS-ZnONPs had ≈1.6, ≈3.0, and ≈3.0 antibacterial activity against E. coli, S. aureus and M. luteus, respectively.	[131]
CS-AgNP[#]	Ag	–	5 – 50 nm[§]	–	S. aureus, P. aeruginosa, E. coli	• CS-AgNPs cross-linked with genipin showed significant antimicrobial activities and inhibition of bacterial growth. • The highest antimicrobial activity was observed in P. aeruginosa (ZOI≈4 mm), followed by E. coli (ZOI≈3 mm) and S. aureus (ZOI≈2 mm).	[132]
CS-SeNP[#]	Se	–	55 – 500 nm[*]	–	S. aureus, MRSA, E. coli	• No significant antimicrobial activity against E. coli. • CS-SeNPs achieved up to 52% growth inhibition in S. aureus and 54% growth inhibition in MRSA.	[133]

(*continued on next page*)

Table 1 (*continued*)

NP formulation	Active ingredient	Encapsulation efficiency	Size	Surface charge	Microbe	Key findings	Ref.
PVA/CS-AgNP[#]	Ag	–	190 – 200 nm[†,§]	–	S. aureus, P. aeruginosa, E. coli, M. luteus S. enterica, S. typhimurium, B. cereus, E. faecalis	• Higher $AgNO_3$ concentrations in PVA/CS-AgNPs led to higher antibacterial activity. • PVA/CS-AgNPs showed highest inhibitory activity against S. aureus (ZOI=21 ± 1 mm) and M. luteus (ZOI=20 ± 0.5 mm). • PVA/CS-AgNPs showed the lowest inhibitory activity against E. coli (ZOI=13 ± 0.5) and S. typhimurium (ZOI=10 ± 0.1)	[134]
COS-AgNP[#]	Ag	–	15.70 ± 4.73 nm[§]	–	S. aureus, E. coli	• A significantly larger ZOI was observed in plates treated with COS-AgNPs than AgNPs. • Inhibition ratio of S. aureus treated with COS-AgNPs and AgNPs were ≈100% and ≈90%, respectively, after about 5 h. • Inhibition ratio of E. coli treated with COS-AgNPs and AgNPs were ≈80% and ≈60%, respectively, after about 5 h.	[123]
2-mercapto-1-methylimidazole (MMT)-CS-AuNp[#]	Au	–	10.07 ± 2.34 nm[†]	-	S. aureus, MRSA, E. coli	• MMT-CS-AuNPs had similar inhibition ratios (between 90% - 100%) as ampicillin for S. aureus and E. coli. • MMT-CS-AuNPs (>90%) had a significantly higher inhibition ratio than ampicillin for MRSA (10% – 20%).	[135]
CS-AgNP[#]	Ag	–	22.80 nm[†]	−45.90 mV	E. coli	• CS- AgNP-loaded CS films (62.22% ± 0.91%) produced the highest E. coli inhibition as compared to CS-AgNP solution (58.52% ± 0.52%), blank CS film (16.67% ± 0.91%), and CS solution (29.63% ± 1.05%).	[124]
CS-AgNP[#]	Ag	–	225.30 nm[†]	−21.40 mV	S. aureus, P. aeruginosa	• The MIC of CS-AgNPs (2.98 µg/ml) were significantly lower than unmodified AgNPs (4.68 µg/ml) and CS alone (3.10 µg/ml) against S. aureus. • The MIC of CS-AgNPs (1.92 µg/ml) were significantly lower than unmodified AgNPs (3.5 6 µg/ml) and CS alone (2.84 µg/ml) against P. aeruginosa.	[136]
CS-AgNP[#]	Ag	–	10 – 30 nm[§]	–	MRSA	• There was no significant difference in bactericidal activity against MRSA between CS-AgNPs, PVP-AgNPs, and AgNPs with all of them achieving 100% bactericidal activity at 8 µg/ml and having an IC50 of about 4 µg/ml.	[137]
CS-SER-AgNP[#]	Ag	–	96.93 ± 0.50 nm[†]	−0.42 ± 0.12 mV	S. aureus, MRSA, P. aeruginosa, S. epidermis, A. baumannii	• CS-SER-AgNPs (31.24 ± 0.43 mm & 29.17 ± 0.41 mm) had larger ZOIs than CS-AgNPs (15.33 ± 0.25 mm & 23.33 ± 0.58 mm) when tested against MRSA and P. aeruginosa, respectively. • CS-SER-AgNPs (11.25 ± 0.43 mm & 13.75 ± 0.43 mm) had smaller ZOIs than CS-AgNPs (27.00 ± 0.78 mm & 16.75 ± 0.50 mm) when tested against S. aureus and A. baumannii, respectively. • CS-SER-AgNPs (22.50 ± 0.53 mm) had similar ZOIs as CS-AgNPs (22.00 ± 0.76 mm) when tested against S. epidermis.	[138]

(*continued on next page*)

Table 1 (*continued*)

NP formulation	Active ingredient	Encapsulation efficiency	Size	Surface charge	Microbe	Key findings	Ref.
CS-SER-AgNP[#]	Ag	–	239.90 ± 1.56 nm[†]	+37 ± 3.6 mV	S. aureus, E. coli	• The ZOI of CS-SER-AgNPs (21.00 ± 1.50 mm) was larger than AgNPs (8.00 ± 1.50 mm) when tested against E. coli. • The ZOI of CS-SER-AgNPs (17.00 ± 1.45 mm) was larger than AgNPs (7.00 ± 1.00 mm) when tested against S. aureus.	[139]
CS-AgNP[#]	Ag	–	10 – 50 nm[§]	–	MRSA, P. aeruginosa	• MIC of CS-AgNPs (1.84 ± 0.17 µg/ml & 3.78 ± 1.70 µg/ml) were significantly lower than unmodified AgNPs (2.65 ± 1.40 µg/ml & 4.89 ± 1.80 µg/ml) and CS alone (3.84 ± 1.80 µg/ml & 5.10 ± 2.20 µg/ml) against P. aeruginosa and MRSA, respectively. • ZOI of CS-AgNPs (20 ± 0.2 mm & 18 ± 0.6 mm) were significantly higher than unmodified AgNPs (10 ± 0.9 mm & 9 ± 1.1 mm) and CS alone (12 ± 0.4 mm & 10 ± 1.8 mm) against P. aeruginosa and MRSA, respectively.	[140]
TMC-immobilised AgNP [‡]	Ag	–	–	–	S. aureus, P. aeruginosa, E. coli	• Sponges loaded with TMC-immobilised AgNPs displayed antibacterial effects against S. aureus (ZOI≈7 mm), P. aeruginosa (ZOI≈8 mm), and E. coli (ZOI≈7 mm). • TMC and CS sponges did not show any antibacterial activity.	[110]

[a] Prepared using ionic gelation method with TPP as a cross-linker;.
[b] Prepared using ionic gelation method with carboxymethyl-β-cyclodextrin (CM-β-CD);.
[c] Prepared by gelation of CS and gelatin mixture;.
[d] Prepared using ionic gelation method with a mixture of CMCS and OH30;.
[e] Prepared using electrostatic droplet method;.
[‖] Prepared using precipitation method;.
[#] Prepared using chemical reduction method;.
[‡] Prepared using template method;.
[†] Size measured using dynamic light scattering (DLS);.
[¶] Size measured using scanning electron microscopy (SEM);.
[§] Size measured using transmission electron microscopy (TEM);.
[*] Method used unspecified.

tested for both bacterial strains [113]. Other studies have also described lower minimum inhibitory concentration (MIC) values for CS against P. aeruginosa as compared to S. aureus [114]. Generally, there are conflicting results in the current literature surrounding the effects of CS against P. aeruginosa and S. aureus as there have been some studies showing the opposite to occur as well [115]. In principle, the most profound antibacterial activity of CS is thought to be derived from the electrostatic interactions between the cationic polymer with the negatively charged bacterial cell wall [116]. In accordance with this, Gram-negative bacteria have been proposed to be more susceptible to the antibacterial effects of CS as they have a larger negative charge than Gram-positive bacteria due to their lipopolysaccharide (LPS)-rich outer membrane [116]. Further supporting this idea is a study by Raafat et al. which reported a S. aureus mutant strain lacking any negatively charged teichoic acid on the cell wall displaying significant resistance against CS [117]. Meanwhile, a S. aureus mutant strain which carried a higher negative charge due the lack of the D-alanine modification in teichoic acids had an increase in susceptibility by about 100 times [117]. Nevertheless, there are a number of studies with evidence suggesting otherwise; whereby the antibacterial effects of CS are more prominent against Gram-positive bacteria [116]. The antibacterial nature of CS most likely stems from a complex combination of events which collectively contribute to bacterial cell death [117]. To truly understand the reasoning behind the different extents in antibacterial activity of CS against Gram-negative and Gram-positive bacteria, more evidence surrounding its possible modes of action will need to be uncovered.

Meanwhile, another study described the antibacterial effects of CSNPs in combination with a first-generation cephalosporin, cefadroxil (CDX) [118]. Wounds treated with *in situ* gels containing CDX-loaded CSNPs had more than 60% inhibition of S. aureus growth, as compared to gels only containing CDX which had about 40% inhibition [118]. These

Table 2 – Summary of wound healing studies evaluating the antimicrobial properties of CS-based NPs and CS-modified metal NPs *in vivo* and *ex vivo*.

NP formulation	Active ingredient	Encapsulation efficiency	Diameter	Surface charge	Wound model (Microbe)	Key findings	Ref.
Therapeutic compound loaded CS-based NPs							
Lecithin-coated CSNP[a]	TGC	22%	235 ± 20 nm[†]	19 ± 5 mV	*Ex vivo* porcine skin (S. aureus)	• S. aureus survival rate was decreased by approximately 2-fold in the presence of TGC-loaded lecithin-coated CSNPs. • CFUs were markedly lower for CSNPs as compared to lecithin-coated CSNPs.	[125]
CSNP[f]	CDX	84.25% ± 0.02%	408.30 ± 53.17 nm[†]	+22.80 ± 0.57 mV	*In vivo* wound infection (S. aureus)	• Inhibition percentage in the CDX-loaded CSNP group was consistently 20% higher than the CDX group, up to Day 4. • Greater than 90% inhibition was obtained in the CDX-loaded CSNP group on Day 5.	[118]
CS-modified metal NPs							
CS-AgNP[#]	Ag	–	15 nm[§]	–	*In vivo* burn wound (No specific bacterial species)	• Wounds treated with CS-AgNPs (≈2.8Log CFU/cm^{-2}) had significantly lower bacterial counts than untreated wounds (≈3.6Log CFU/cm^{-2}) and SSD-treated wounds (≈3.6Log CFU/cm^{-2}). • Bacterial counts for CS-AgNP treated wounds were about 7–10 times less than SSD treated wounds.	[141]
CS-AgNP[#]	Ag	–	10 - 30 nm[§]	–	*In vivo* infected full-thickness wound (MRSA)	• Similar antibacterial effects were observed for uncoated AgNPs, PVP-AgNPs, and CS-AgNPs. • MRSA was not detected in all treatment groups beyond day 3 post-wounding.	[137]

[a] Prepared using ionic gelation method with TPP as a cross-linker;.
[f] Prepared using W/O/W type double emulsification;.
[#] Prepared using chemical reduction method;.
[†] Size measured using DLS;.
[§] Size measured using TEM

observations show the enhanced antibacterial effect which can be achieved when using CSNPs in combination with an antibiotic.

The antimicrobial activity of CSNPs for wound healing applications have also been studied in combination with natural active constituents. A thorough study evaluating the synergistic effects of CSNPs and Homalomena pineodora (H. pineodora) essential oil against clinical isolates of common diabetic wound pathogens has been reported [119]. The study found that CSNPs loaded with H. pineodora essential oil exhibited synergism (Fractional inhibitory concentration, FIC indices ≤ 0.5) against S. aureus, B. cereus, B. subtilis, methicillin-resistant S. aureus (MRSA), P. mirabilis, A. anitratus, S. boydii, and C. albicans [119].

7.2.2. *Carboxymethyl NPs*

Two separate studies by Sun et al. and Zou et al. reported the use of CMCSNPs together with a bioactive OH–CATH30 (OH30) peptide for the purpose of wound healing [120,121]. In contrast to CS-based NPs, CMCSNPs typically carry an overall negative charge due to the presence of carboxylic acid functional groups instead of amino groups. The negatively charged OH30-loaded CMCSNPs incorporated into polyvinyl alcohol (PVA)/CS nanofibres reported by Zou et al. produced significant antimicrobial activity against both S. aureus and E. coli when compared to unloaded PVA/CS nanofibres, with a larger difference observed against E. coli. [121]. In another study, unloaded CS-coated CMCSNPs only had modest inhibitory activity against E. coli with less than 50% inhibition, which decreased over time. However, the OH30-loaded CS-coated CMCSNPs exhibited 100% inhibition which was sustained over 24 h [120]. Interestingly, the authors of this study compared the effects of negatively charged OH30-loaded CMCSNPs (zeta potential, $\zeta = -36.7 \pm 3.3$ mV) with positively charged OH30-loaded CS-coated CMCSNPs (zeta potential, $\zeta = +30.2 \pm 5.1$ mV) [120]. The positively charged OH30-loaded CMCSNPs had significantly greater antibacterial effects than their negatively charged counterparts [120]. Findings from this study further highlight the importance of particle surface charge on the antibacterial effects even when being used as

a delivery vehicle for antimicrobial compounds such as the OH30 peptide.

7.2.3. CS-modified metal NP

CS-modified metal NPs, particularly CS-AgNPs have been widely studied for their antimicrobial wound healing applications [122]. PVA/COS-AgNPs were compared with PVA/COS/$AgNO_3$ and unloaded PVA/COS nanofibres in terms of their antimicrobial activity against S. aureus and E. coli [123]. In this study, the unloaded PVA/COS nanofibres exhibited the lowest antimicrobial activity with no noticeable zone of inhibition (ZOI) [123]. On the other hand, the PVA/COS-AgNP group produced the greatest antimicrobial activity, with an inhibition ratio of 100% against S. aureus and an inhibition ratio greater than 80% against E. coli after 5 h of incubation [123]. In contrast, PVA/COS/$AgNO_3$ only had an inhibition ratio of greater than 80% for both bacteria after 5 h of incubation and a smaller inhibition zone than PVA/COS-AgNPs [123]. Similar findings were reported in a study evaluating the antimicrobial activity of CS-AgNPs and CS solution alone [124]. The CS-AgNPs had an average ZOI diameter of 5.27 cm and 58.52% inhibition while CS solution alone only had an average ZOI diameter of 2.67 cm and 29.63% inhibition when tested against E. coli, demonstrating superior antimicrobial effects by CS-AgNPs [124]. When used in combination with other materials with intrinsic antimicrobial properties such as transition metals, antibiotics or natural products, CSNPs, CMCSNPs and CS-modified metal NPs are capable of producing enhanced antimicrobial effects [111].

7.3. Oxidative stress and anti-oxidative properties

7.3.1. CSNPs

The formation of CSNPs with or without other active ingredients may take advantage of the mild anti-oxidative properties of CS to further improve wound healing outcomes by preventing excessive oxidative stress around the wound area.

A study by Sami et al. reported very little to no significant antioxidant activity in the tested CSNPs [112]. Interestingly, this study used a modified 4,5-dimethylthiazole-2-yl)−2,5-diphenyltetrazolium bromide (MTT) assay without any cell cultures [112]. Only the reagent and experimental treatments were used on the formulated CSNPs to quantify its antioxidant activity [112]. The most common application of MTT lies in determining cell viability, proliferation, and cytotoxicity instead of antioxidant activity [142]. In this scenario, the basic principle of the assay was employed, whereby the soluble MTT reagent is reduced to insoluble formazan by nicotinamide adenine dinucleotide phosphate (NADPH) produced by cell metabolism [112,142]. This was used by the authors to quantify the reduction of MTT by the antioxidant, CSNP, in the absence of any cells [142]. There is currently limited evidence to support the reliability of an MTT assay in quantifying antioxidant activity in comparison to more commonly used assays such as the DPPH free radical scavenging method [142]. Therefore, the findings could be further investigated with other commonly used antioxidant assays for validation purposes.

Gallic acid (GA) is a plant polyphenol known for having potent antioxidative properties. The antioxidative properties of GA-loaded CSNP incorporated into collagen-fibrin scaffolds were evaluated for the purpose of wound healing [143]. Authors of this study compared the DPPH scavenging activity of collagen-fibrin scaffolds containing GA-loaded CSNPs against unloaded collagen and collagen-fibrin scaffolds [143]. The antioxidant activity was found to increase substantially to about 90% with the addition of GA-loaded CSNPs in comparison to the unloaded collagen and collagen-fibrin scaffolds which only produced about 10% antioxidant activity [143]. Combination of the highly potent antioxidant, GA with the mildly antioxidative CSNPs resulted in a significant boost in antioxidant activity higher than each of these components on their own. [143]. An interesting note is when GA is conjugated to CS as GA-grafted-CS, but not formulated as NPs, the antioxidative effects from DPPH, 2,2′-azino-bis(3-ethylbenzothiazoline-6-sulfonic acid) (ABTS), and oxygen radical scavenging assays were lower than or equal to GA alone [144]. However, when GA is encapsulated in CSNPs in a different study, the antioxidative effects were increased above GA alone [143,144].

Mangiferin-loaded CSNPs were similarly observed to strengthen the free radical scavenging effect of mangiferin in a separate study by Samadarsi and Dutta [145]. Statistically higher antioxidative effects were seen in DPPH, ferric reducing antioxidant power (FRAP), and ABTS assays when comparing mangiferin-loaded CSNPs to mangiferin alone [145]. The same was observed for naringenin-loaded CSNPs compared to naringenin alone whereby higher hydroxyl, DPPH, and nitrite free radical scavenging activity was obtained in the former group [146]. These studies had all used the ionic gelation method with TPP as the cross-linker to prepare the CSNPs [143,145,146]. NP sizes and surface charges determined by dynamic light scattering (DLS) in these studies ranged from 91.0 nm to 446.7 nm and +22.0 mV to +58.4 mV, respectively [143,145,146]. Encapsulation efficiency of these natural compounds were also found to range between 73% to 85% [143,145,146]. The differences in active compound tested in each of these studies limit the comparison of beneficial CSNP effects in relation to these important properties. Moreover, notice should be taken regarding the range of particle size, surface charge, and encapsulation efficiency reported in these studies, which could all influence the effects of the CSNPs, leading to the observed findings.

7.3.2. CS-modified metal NPs

Results from a study using CS-AgNPs showed that an increased incubation time of 1 h to 24 h consistently improved the scavenging rate of CS-AgNPs by about 5% across all tested concentrations [141]. The CS-AgNPs also showed a dose-dependent increase in scavenging rate which gradually increased from about 70% at 0.004 ng/ml to about 85% at 0.13 ng/ml [141]. Meanwhile, Haiji et al. thoroughly examined the antioxidant properties of PVA/CS-AgNPs compared to CS alone using both *in vitro* and *in vivo* techniques [134]. Significant antioxidant activity from PVA/CS-AgNPs was observed, which was comparable to butylated hydroxyanisole (BHA) and L-mannitol that were used as positive controls [134]. CS alone had lower antioxidant activity than PVA/CS-

AgNPs in all of the *in vitro* antioxidant assays [134]. The *in vivo* assay revealed increased expression of antioxidative enzymes, namely catalase (CAT), superoxide dismutase (SOD), glutathione peroxidase (GPx) following treatment with PVA/CS-AgNPs in comparison to the control group [134]. Lower levels of lipid peroxidation were also reported for wounds treated with PVA/CS-AgNPs when compared to the control group [134]. Overall, the findings from these studies indicate that CSNPs and CS-modified metal NPs are capable of producing antioxidative effects which may be beneficial to wound healing.

7.4. *Inflammatory response regulation*

7.4.1. *CSNPs*

Formulation of CSNPs from different types of CS polymers were shown to improve the permeation and distribution of CS across the wound site and increase the internalisation of CS by macrophages [147]. This may lead to more profound effects observed in CSNPs than unmodified CS, as they have easier access to target cells in terms of regulation of immune responses.

An *in vitro* study involving LPS-treated RAW264.7 cells had reported significant decrease of IL-6 and TNF-α expression following treatment with CUR-loaded CSNPs and free CUR alone in a dose-dependent manner [148]. The downregulation of both pro-inflammatory cytokines was significantly greater in the CUR-loaded CSNP group than the free CUR group [148]. CUR-loaded CSNPs were able to significantly reduce the inflammation produced by LPS-stimulated macrophages *in vitro* [148]. A separate study investigated the effects of vaccarin (VAC), VAC-loaded CSNPs, and unloaded CSNPs on the expression of TNF-α and IL-1β in an *in vivo* full-thickness excisional wound model [149]. Findings from this study suggested that VAC-loaded CSNPs were capable of up-regulating the expression of IL-1β [149]. Another interesting result obtained from this study was a significantly elevated level of TNF-α in VAC-treated wounds which was not observed in any other groups, including the VAC-loaded CSNP group [149]. Similarly, Choudhary et al. had reported a markedly lower expression of TNF-α in wounds treated with quercetin (QUE)-loaded CSNPs when compared to wounds treated with bulk QUE alone [150]. Meanwhile, the anti-inflammatory IL-10 and TGF-β1 were significantly elevated in wounds treated with QUE-loaded CSNPs when compared to control wounds and QUE-treated wounds [150]. Authors in these three studies utilised the ionic gelation method with TPP as the cross-linker to synthesize the CSNPs [148–150]. The NP sizes ranged from 91.3 nm to 361.2 nm across the three studies [148–150]. Only Hou et al. had reported the zeta potential of the VAC-loaded CSNPs, which averaged at +37.1 mV [149]. Collectively, these results highlight the important role of CSNPs as drug delivery vehicles for regulating inflammation during wound healing, improving the effects of the active ingredients when delivered in CSNPs.

7.4.2. *CMCSNPs*

In a study evaluating OH30-loaded CMCSNPs coated with a layer of CS, elevated levels of TNF-α were reported in wounds treated with OH30 alone while lower levels were observed in wound treated with OH30-loaded CMCSNPs coated with CS [120]. Other pro-inflammatory cytokines, IL-6 and IL-8 were initially expressed at higher levels in OH30-loaded CS-coated CMCSNP-treated wounds but steadily declined to levels lower than or similar to untreated wounds [120]. OH30-loaded CS-coated CMCSNPs also displayed a longer sustained increase in IL-10 expression than OH30 alone, but a consistently lower expression of TGF-β1 than untreated wounds throughout the study duration [120]. NPs formulated in this study had an average size of 258.7 nm and the outer layer of CS coating the CMCSNPs granted a positive surface charge of +30.2 mV [120]. The particle size and surface charge of the CS-coated CMCSNPs in this study are similar to those reported for the studies on CSNPs previously discussed.

The effect of CSNPs and CMCSNPs carrying different types of therapeutic agents produced varying results in terms of the expression of pro- and anti-inflammatory cytokines. This highlights the complex interactions between the CSNPs and CMCSNPs together with their therapeutic cargo with the surrounding immune cells during the inflammatory phase. It was interesting to note that in three separate *in vivo* studies involving VAC, QUE, and OH30, CSNPs and CS-coated CMCSNPs were able to reduce the expression of TNF-α which was significantly elevated in treatment groups involving the active therapeutic compounds alone [120,149,150]. The diverse effects of CSNPs and CMCSNPs on these cytokines during wound inflammation can be further connected to other effects observed, such as in collagen deposition or angiogenesis due to the varied nature of these cytokines.

7.4.3. *CS-modified metal NPs*

Significantly lower levels of IL-1β mRNA expression following treatment with CS-AgNP was reported in an *in vivo* burn wound study [141]. The levels reported were lower than both the control group and positive control group with silver sulfadiazine (SSD) as the treatment throughout the duration of the study [141]. In contrast, TGF-β1 mRNA expression appeared to be significantly higher in wounds treated with CS-AgNPs than in control wounds and SSD-treated wounds, but only on day 7 [141]. This could be due to the fact that CS-AgNP treated wounds had achieved almost complete closure by day 7, which explains the possible peak in TGF-β1 expression at this point [141]. Other treatment groups experienced an elevation in TGF-β1 mRNA at later timepoints where the levels in the CS-AgNP group began declining as the wound healed earlier [141]. Overall, the results from this study showcased the ability of CS-AgNPs to act as an anti-inflammatory agent by modulating both IL-1β and TGF-β1 levels [141].

7.5. *Angiogenesis and new vessel formation*

7.5.1. *CSNPs*

The relationship between CS and angiogenesis is not as clearly described in the current literature as its other properties. Minor effects of CS on angiogenesis are attributed to its indirect mechanisms on inflammation and oxidative stress [148]. Angiogenesis is initiated by a hypoxic wound environment, the release of pro-angiogenic growth factors, and the release of proteases [151,152]. This helps to deliver nutrient-rich blood to sustain the regeneration of skin tissue

and ECM around the wound bed [151,152]. Nevertheless, excessive levels of angiogenesis have been linked to hypertrophic scar formation. Hence, optimal wound healing outcomes require a healthy level of angiogenesis [153]. Numerous studies have investigated the application of CS and its derivatives in formulating drug delivery systems for pro-angiogenic uses in wounds [154,155].

The difference in angiogenic effect of CS and CSNPs on human umbilical vascular endothelial cells (HUVEC) were examined by Wang et al. [75]. It was revealed that calcium alginate hydrogels containing CSNPs produced significantly higher cell migration, tubule formation, and VEGF expression in HUVEC as compared to CS-calcium alginate hydrogels [75]. A significant increase in ROS production was observed in HUVEC treated with calcium alginate hydrogels containing CSNPs in comparison to CS-calcium alginate hydrogels [75]. In addition, when cells were treated with calcium alginate hydrogels containing CSNPs together with a strong antioxidant, N-acetyl cysteine (NAC), the ROS production dropped to levels similar to control cells [75]. This combination of calcium alginate containing CSNPs with NAC also did not show any significant changes in HUVEC migration, tubule formation, or VEGF expression, suggesting the possible role of ROS upregulation by CSNPs in facilitating angiogenesis [75]. The authors attributed the differences in the results between CSNPs and unmodified CS to the enhanced cellular uptake of CSNPs [75].

In a separate *in vitro* study, CUR-loaded CSNPs were evaluated using high glucose induced HUVEC (HG-HUVEC) and RAW264.7 to mimic diabetic wound conditions [148]. Following treatment with CUR-loaded CSNPs and CUR alone, an increased HG-HUVEC cell migration, tubule formation, and VEGF expression was observed in cultures incubated together with RAW264.7 and LPS [148]. The increased cell migration, tubule formation, and VEGF expression was observably higher in CUR-loaded CSNPs than CUR alone. In this study, the angiogenic effects of CUR-loaded CSNPs and CUR alone were explained based on their ability to reduce RAW264.7 induced inflammation [148]. This was supported by their findings whereby a high concentration of CUR-loaded CSNPs was able to restore HG-HUVEC migration, tubule formation, and VEGF expression to values similar to HG-HUVEC incubated without RAW264.7 and LPS [148]. CUR-loaded CSNPs were also shown to elevate the number of blood vessels in a separate *in vivo* wound healing study by more than two times when compared to untreated wounds [156]. When used in combination with a polymeric fibre mat, CUR-loaded CSNPs further increased the number of blood vessels formed as compared to using the polymeric fibre mat alone [156].

Both of these studies synthesised CUR-loaded CSNPs using the ionic gelation method with TPP as the cross-linker [148,156]. Although using the same preparation method and similar CS polymers in terms of MW and DDA, the properties of CUR-loaded CSNPs in these studies largely differed. The first study reported an average particle size of 91.3 nm while the second study had a size of 359.0 nm [148,156]. Although zeta potential was only reported in the second study as −12.2 mV, the first study claimed their CUR-loaded CSNPs to have an overall positive surface charge [148,156]. Drug loading and encapsulation efficiency also largely differed, as the first study had a drug loading of 35.1% and encapsulation efficiency of 77.2% while the second study had 4.2% and 93.0% as the drug loading and encapsulation efficiency, respectively [148,156]. These differences highlight the importance of the preparation steps involved in synthesising CSNPs, such as the ratio of each component along with the purification method. However, despite the vastly different NP properties reported, positive outcomes were still achieved by both authors, which further inform us on the degree of flexibility allowed by CSNPs carrying specific compounds in exerting their effects.

Using a scratch assay, Hou et al. reported an increase in HUVEC migration rate for cells treated with VAC, VAC-loaded CSNPs, and unloaded CSNPs; whereby the largest increase was observed with VAC, followed by VAC-loaded CSNPs and unloaded CSNPs [149]. However, a larger number of migrated cells were seen in the VAC group than the VAC-loaded CSNP group when using the transwell cell migration assay [149]. Both groups exhibited higher cell migration rate than untreated cells in the same assay [149]. Furthermore, findings from the same study showed that wounds treated with VAC and VAC-loaded CSNPs both produced significantly higher levels of microvascular density (MVD) in wound tissues as compared to the control group [149]. Platelet-derived growth factor (PDGF)-BB expression of wounds treated with VAC and VAC-loaded CSNPs peaked and declined earlier than control wounds [149]. The outcomes from this study provide evidence that CSNPs are suitable as a delivery vehicle for VAC in supporting healthy angiogenesis in wounds which is beneficial for tissue regeneration.

QUE-loaded CSNPs used in an *in vivo* study were also shown to be able to increase the VEGF expression in wound tissues [150]. The increase in VEGF expression was higher than the levels obtained from QUE-treated wounds and control wounds [150]. Interestingly, an inverse relationship was observed between the increase in VEGF expression and QUE concentration in QUE-loaded CSNPs [150]. A similar inverse relationship was seen upon histological analysis of blood vessel density between the concentration of QUE in QUE-loaded CSNPs and the number of blood vessels on day 7 of treatment. However, on day 21, this was reversed whereby increasing QUE concentration in QUE-loaded CSNPs led to an increase in number of blood vessels counted. This contrasts the results obtained from a study by Kant et al. whereby VEGF mRNA expression in wound tissues increased following increases in QUE concentration dissolved in DMSO [157]. The QUE concentrations used in these two studies were similarly reported as 0.03%, 0.1% and 0.3% [150,157]. The differences in the findings from these studies may be due to the differences in drug release kinetics and skin permeation offered by QUE-loaded CSNPs as compared to QUE alone applied topically to the wound. Further research into the possible reasons for this observation is required before a clear explanation can be drawn.

Despite the positive results obtained in the *in vitro* studies using HUVEC under different conditions, the effects of unloaded CSNPs on angiogenesis using *in vivo* models, in terms of VEGF and PDGF-BB expression, were not as noticeable [75,148-150,158,159]. However, when used alongside another active compound, these formulations were capable of producing promising results with higher

expressions of pro-angiogenic biomarkers and increased angiogenesis activity which peaked earlier and declined sooner than control groups [148-150,159].

7.5.2. CNPs

An interesting result obtained by a study measuring the effects of CNPs on neovascularisation revealed that CNP-based aerogels produced the highest amount of neovascularisation in wound tissues on Day 7 of treatment and the lowest amount of neovascularisation on day 14 [158]. The difference in neovascularisation in comparison to all other groups were significantly large [158]. This finding is suggestive of a wound dressing capable of accelerating the wound healing process by facilitating the growth of new vessels earlier without causing excessive growth of vessels at later stages which may cause unwanted outcomes such as hypertrophic scarring [158]. Formation of more structurally mature and larger-sized blood vessels was also observed in CNP-based aerogels in comparison to other groups [158]. This further supports the use of CNPs which enhance the development of blood vessels in wounds in a timely manner without impeding the maturity or structural integrity of newly formed vessels.

7.5.3. CS-modified metal NPs

Li et al. had also reported an increase in VEGF mRNA expression in full-thickness incisional wounds treated with PVA nanofibres containing COS-AgNP which peaked earlier than control wounds and achieved baseline levels quicker than control wounds [159]. The elevation in VEGF mRNA expression was only observed to be statistically significant on Day 7 and 9, while the other time points were not statistically significant [159]. A trend was also noticed whereby the PVA/COS-AgNP nanofibre group displayed an earlier and higher peak in VEGF mRNA than all the other groups which subsequently declined sooner [159]. This is a desirable observation as it depicts quicker vascularisation which generally speeds up wound regeneration. Treatment of wounds with PVA/COS-AgNP together with a TGF-β1 inhibitor produced the slowest but similarly high peak in VEGF mRNA which remained slightly elevated at the study end-point [159]. Authors of this study connected this observation with the wound healing time observed for this treatment group, which was similarly the slowest, and attributable to a slower formation of granulation tissue [159]. This further highlights the intricacy of angiogenesis as part of the wound healing process, where the expression of growth factors can be easily changed by the expression and action of other cytokines.

7.6. Collagen deposition

7.6.1. CSNPs

Reconstruction and reorganization of the ECM are two separate but intertwined processes which are vital for successful wound healing [160,161]. Of the many different components of the ECM, collagen has an important role of maintaining the structural and dynamic integrity of the ECM while serving as a scaffold for other biological processes [160,161]. During the proliferative phase of wound healing, collagen type III is typically present in greater amounts whereas during the remodeling phase, collagen type I becomes dominant in scar tissue [160–163]. Hydroxyproline is an amino acid which has been commonly used as a means to estimate the amount of collagen due to its high content in collagen [164,165].

A noticeable trend of increasing hydroxyproline content to varying degrees in wounds treated with different CSNPs, CMCSNPs, and CS-modified metal NPs were observed across a number of studies (Table 3). Kaparekar et al. measured the changes in collagen content of wound tissues through estimation using hydroxyproline [143]. The study found that treatment of wounds with GA-loaded CSNPs impregnated into polymeric scaffolds resulted in elevated collagen deposition on Day 4, 8 and 12 when compared to empty polymeric scaffolds and untreated wounds [143]. The increase in collagen content were statistically significant on Days 4 and 8 [143]. Findings from a study using polycaprolactone (PCL)-gelatin scaffolds containing CUR-loaded CSNPs had showed that the treatment of wounds with CUR-loaded CSNPs produced significantly higher collagen content in wound tissues than control and vehicle control groups [156]. Furthermore, this study had also showed a mild increase in collagen content for wounds treated with blank CSNP-loaded PCL-gelatin scaffolds alone [156].

However, melatonin (MEL)-loaded lecithin/CSNPs did not produce an increase in collagen content in one study by Lopes Rocha Correa et al. [166]. No significant difference in collagen density was observed with MEL-loaded lecithin/CSNP treatment in comparison to other groups as reported by the authors [166]. Although not significant, there was an increase in collagen observed in MEL-loaded lecithin/CSNP groups compared to the vehicle formulation group [166]. Particle size, surface charge, and encapsulation efficiency of the NPs used in this study can be seen in Table 3. The MEL-loaded lecithin/CSNPs with no statistically significant findings did have a considerably lower encapsulation efficiency than the other two studies discussed earlier [166]. This may be a possible factor in the lack of substantial difference observed, along with the slower release of MEL from the NPs which was highlighted by the authors [166].

7.6.2. CMCSNPs

In a study by Sun et al., OH30-loaded CS-coated CMCSNPs did not increase the collagen content of wounds following treatment [120]. In fact, OH30-loaded CS-coated CMCSNPs had been shown to produce a significantly lower collagen content as compared to control [120]. It also had the lowest amount of collagen type I and the highest amount of collagen type III when compared to the control group, blank CMCSNP treatment group, and OH30 treatment group [120]. A low collagen type I to collagen type III ratio is typically synonymous with slower wound remodeling while higher ratios have been related to faster wound healing and maturation [120]. This study had explained the contrasting results from the wound closure observed and the collagen type I to type III ratio by the appearance of hypertrophic scarring [120]. Photographs of the wound at the study end-point had showed clear results of less scarring on the surface of the closed wound for the OH30-loaded CMCSNP

Table 3 – Summary of wound healing studies evaluating the effects of CS-based NPs, CMCSNPs, CNPs, and CS-modified metal NPs on collagen deposition.

NP formulation	Active ingredient	Encapsulation efficiency	Diameter	Surface charge	Wound model (Animal)	Key findings	Ref.
Therapeutic compound loaded CS-based NPs							
CSNP[a]	GA	73.20% ± 2.10%	252.90 ± 3.09 nm[†]	+33.50 ± 0.30 mV	Excision wound (Male Wistar rat)	• Collagen and hexosamine content were the highest in the collagen-fibrin scaffold containing GA-loaded CSNP treatment group (≈0.4 mg/100 mg dry weight) as compared to the control group (≈0.25 mg/100 mg dry weight) and unloaded collagen-fibrin scaffold treatment group (≈0.3 mg/100 mg dry weight).	[143]
CSNP[a]	CUR	93.00% ± 5.00%	359 ± 65 nm[†]	−10.70 ± 0.10 mV	Full-thickness wound (Male Wistar rat)	• Highest collagen density was obtained in the PCL-gelatin containing CUR-loaded CSNP group (49.6% ± 5.6%) • Control group and PCL-gelatin group had collagen densities of 7.6% ± 3.0% and 12.1% ± 3.2%, respectively.	[156]
Lecithin/CSNP[g]	MEL	27%	160.43 ± 4.45 nm[†]	+25.00 ± 0.57 mV	Diabetic full-thickness wound (Wistar rat)	• No significant difference in collagen content was observed between MEL-loaded lecithin/CSNP (≈50.7), MEL alone (≈63.0), blank lecithin/CSNPs alone (≈44.8), and the vehicle control group (≈43.5).	[166]
CMCSNPs							
CMCS-OH30 NP[d]	OH30	82.46% ± 1.11%	258.70 ± 13.30 nm[†]	+30.20 ± 5.10 mV	Full-thickness wound (Female Kunming mice)	• Wounds treated with OH30-loaded CMCSNPs had a collagen I/collagen III ratio of 1.875 while control wounds had a collagen I/collagen III ratio of 12.22. • Highest total collagen content was observed in the control group, followed by the blank CMCSNP group, OH30 group, and the OH30-loaded CMCSNP group.	[120]
ChitinNPs							
CNP[g]	–	–	14 ± 3 nm[§]	–	Full-thickness wound (Male Sprague-Dawley rat)	• CNP-based aerogel group (collagen density ≈ 40%) had the highest average collagen density. • CNP-based cryogel group (collagen density ≈ 35%) had similar levels of collagen density as the positive control (DuoDERM®) (collagen density ≈ 35%). • The control group only had a collagen density of approximately 20%	[158]
CS-modified metal NPs							
PVA/CS-AgNP[#]	Ag	–	190 – 200 nm[†,§]	–	Full-thickness wound (Male Wistar rat)	• PVA/CS-AgNPs produced a hydroxyproline content of 27.53 ± 0.47 mg/g which was close to the amount present in the original tissue and was about 1.6 times higher than the control group.	[134]
PVA/COS-AgNP[#]	Ag	–	–	–	Full-thickness wound (Male Sprague-Dawley rat)	• The relative hydroxyproline content in the PVA/COS-AgNP group (≈0.5 by day 3) was significantly higher than the control group (≈0.3 by day 3). • PVA/COS-AgNP group had more rapid collagen I and III formation than the control group.	[159]
CS-AgNP[#]	Ag	–	15 nm[§]	–	Burn wound (Male Sprague-Dawley rat)	• Significantly higher hydroxyproline content was observed in the CS-AgNP group (4.90 ± 0.05 mg/g) as compared to the control (4.59 ± 0.20 mg/g) and SSD (4.57 ± 0.20 mg/g) groups.	[141]

(continued on next page)

Table 3 (*continued*)

NP formulation	Active ingredient	Encapsulation efficiency	Diameter	Surface charge	Wound model (Animal)	Key findings	Ref.
PVA/COS-AgNP[#]	Ag	–	15.31± 4.00 nm[§]	–	–	• HSF cells treated with PVA/COS-AgNP nanofibres (hydroxyproline content = 0.1092) produced significantly higher hydroxyproline than the untreated group (hydroxyproline content = 0.0896).	[167]

[a] Prepared using ionic gelation method with TPP as a cross-linker.
[d] Prepared using ionic gelation method with a mixture of CMCS and OH30.
[g] Prepared using self-assembly.
[#] Prepared using chemical reduction method.
[†] Size measured using DLS.
[§] Size measured using TEM.

treatment group in comparison to other groups [120]. Hence, the significantly higher overall collagen content found in the control group could be a consequence of the increase in scar tissue formation [120].

7.6.3. CNPs

Guo et al. had reported the use of CNP-based aerogels in animal wounds whereby the collagen density present in wound tissues at the study end-point was found to be more than 2 times higher than the amount present in the control group [158]. A similar relative increase in collagen density was also seen in wounds treated with CNP-based aerogel when compared to the control group at the mid-point of the study [158]. The positive control used in this study, DuoDERM®, produced similar levels of collagen density elevation as CNP-based cryogels which were still significantly lower than the levels achieved by CNP-based aerogels on both timepoints [158]. optimization of the biological effects of NPs do not end with the NP formulation itself but extends further to the final formulation design. As shown by Guo et al., formulating CNP into aerogels and cryogels through two different methods resulted in distinct differences in the final biological activity when treating wounds [158].

7.6.4. CS-modified metal NPs

In vitro measurements of hydroxyproline expression in human skin fibroblast (HSF) cells treated with PVA/COS-AgNPs provided evidence of increased hydroxyproline production [167]. A minor dose-dependent effect was observed in cells treated with PVA/COS-AgNPs, an increase in concentration from 12.5 µg/ml to 500 µg/ml led to a small but statistically significant increase in hydroxyproline expression [167]. Addition of a TGF-β1 inhibitor in combination with PVA/COS-AgNPs led to a staggering decrease in hydroxyproline content which was even lower than the control group [167]. This may indicate a dependence on the TGF-β1 signaling pathway for the elevation in hydroxyproline observed following PVA/COS-AgNP treatment. Further supporting this is a similar dose-dependent increase in TGF-β1 expression in cells following PVA/COS-AgNP treatment [167]. In another study, PVA/COS-AgNP formulated in the form of nanofibres was also shown to increase hydroxyproline expression in wound tissues by a statistically significant amount compared to control [159]. This increase was statistically significant from Day 3 to 9 and remained slightly higher than the control group from Day 12 to 18 [159]. Addition of a TGF-β1 inhibitor similarly reduced the effect of PVA/COS-AgNPs to levels similar or less than the control group [159]. This also provides evidence on the relevance of TGF-β1 on the effects of PVA/COS-AgNPs. Oryan et al. had found statistically higher hydroxyproline content in wound tissue following treatment with high dose CS-AgNPs at Day 7 when compared to control [141]. The amount of hydroxyproline was even higher than the positive control group treated with SSD and the low dose CS-AgNP group [141]. Hydroxyproline expression at other time points were similar between each group in the study [141]. Another *in vivo* study demonstrated that the treatment of wounds using PVA/CS-AgNPs had produced hydroxyproline levels which were almost as high as the levels observed in the original tissue and were 1.63 times higher than the amount present in the control group [134]. The increase in hydroxyproline levels in the PVA/CS-AgNPs was very closely similar to the increase seen in the PVA/CS group which was 1.59 times higher than the control group [134]. This observation may indicate that PVA/CS modification may provide a greater contribution to the effects seen than the AgNP component of the formulation.

7.7. *In vitro* wound closure rate acceleration

7.7.1. CSNPs

The final step in wound healing involves re-establishment of the previously broken skin. By facilitating the closure of wounds, overall patient outcomes can be improved, and health care burdens can be reduced tremendously [9].

Studies examining the wound healing effects of CSNPs incorporated with bioactive compounds on fibroblast or keratinocyte cell lines are summarised in Table 4. Improvements in cell migration rates were observed in these cells. Fibroblast cells around the wound, which mature into myofibroblasts, have an important role in wound contraction while keratinocytes are directly involved in forming a new epithelial layer during the process of re-epithelialisation [17,19]. Fibroblast cells treated with CUR-loaded CSNPs and

Table 4 – Summary of studies evaluating the effects of CS-based NPs, CMCSNPs, and CS-modified metal NPs on the *in vitro* cell migration rate using a scratch assay.

NP formulation	Active ingredient	Encapsulation efficiency	Diameter	Surface charge	Cell type	Percentage wound closure	Reference
Therapeutic compound loaded CS-based NPs							
CSNP[a]	CUR	99.93%	279.70 ± 20.30 nm[†]	+52.4 ± 1.50 mV	Human Dermal Fibroblast-Adult (HDFa)	• Control (40.02%) • CSNP (19.86%) • CUR-loaded CSNP (69.39%)	[128]
CSNP[a]	GA	73.20% ± 2.10%	252.90 ± 3.09 nm[†]	+33.50 ± 0.30 mV	Murine Fibroblast (NIH/3T3)	• Control (Incomplete healing) • CSNP (Incomplete healing) • GA-loaded CSNP (Complete healing)	[143]
Lecithin/CSNP[g]	MEL	–	255.00 ± 7.70 nm[†]	+24.50 ± 0.60 mV	Human Keratinocyte (HaCaT)	• Control (27.0% ± 7.2%) • Lecithin/CSNP (44.7% ± 11.8%) • MEL-loaded lecithin/CSNP (59.4% ± 12.5%)	[168]
CMCSNPs							
CMCSNP[d]	OH30	82.46% ± 1.11%	258.70 ± 13.30 nm[†]	+30.20 ± 5.10 mV	Human Keratinocyte (HaCaT)	• Control (≈60%) • OH30 (≈80%) • CMCSNP (≈75%) • OH30-loaded CMCSNP (≈90%)	[120]
Conjugated linoleic acid (LA)-CMCSNP[g]	rhEGF	82.43% ± 3.14%	155.30 ± 4.62 nm[†]	−23.30 ± 0.37 mV	Murine Fibroblast (L929)	• Control (11.27% ± 4.06%) • rhEGF (34.78% ± 2.18%) • rhEGF-loaded LA-CMCSNP (38.62% ± 5.29%)	[169]
CS-modified metal NPs							
CS-AgNP[#]	Ag	–	225.30 nm[†]	−21.40 mV	Murine Macrophage (RAW 264.7)	• $AgNO_3$ (59%) • CS (82%) • CS-AgNP (85%)	[136]

[a] Prepared using ionic gelation method with TPP as a cross-linker.
[d] Prepared using ionic gelation method with a mixture of CMCS and OH30.
[g] Prepared using self-assembly.
[#] Prepared using chemical reduction method.
[†] Size measured using DLS.

GA-loaded CSNPs in two separate studies showed increased rates of migration as compared to untreated cells and cells treated with CSNPs alone [128,143]. Although these studies utilised different cell lines, CUR-loaded CSNPs were found to improve human dermal fibroblast (HDF) cell migration as the scratched wound was fully closed by 48 h following treatment as compared to the control which took 72 h [128]. GA-loaded CSNPs similarly produced faster migration rates in a murine fibroblast cell line, NIH/3T3, whereby treated wounds were fully closed by 24 h while the control group required greater than 48 h [143].

MEL-loaded lecithin/CSNPs were found to improve the migration rate of keratinocyte cells *in vitro* in a study investigating the effects of different MW and DDA of the CS used in the formulations [168]. A higher DDA of greater than 90% and low MW of 50 to 150 kDa were found to be the optimal parameters in designing MEL-loaded lecithin/CSNPs, which provided the best *in vitro* cell migration results on keratinocytes [168]. Changes in MW seem to produce more prominent effects towards cell migration than DDA, as both low MW formulations still produced statistically significant effects despite changes in DDA, whereas the high MW formulations did not produce any substantial increase in cell migration [168]. This may be further due to the smaller particle sizes granted by the lower MW formulations although the differences were minor between formulations.

All three of these studies had closely similar particle sizes and positively charged surfaces (Table 3), especially the GA-loaded CSNPs and the MEL-loaded lecithin/CSNPs which were reported to have average sizes of 252.9 and 255.0 nm, respectively [143,168]. The small particle sizes of NPs used in these studies may be an important factor in achieving these outcomes, as smaller sized particles have a larger surface area to volume ratio to interact with cells more frequently, which may lead to an increase in cellular uptake and other cell-surface interactions.

7.7.2. CMCSNPs

Other studies have also investigated the effects of OH30 and recombinant human epidermal growth factor (rhEGF) when used in combination with CMSNPs on the migratory rates of human keratinocytes and murine fibroblasts [120,169]. CS-coated CMCSNPs ferrying OH30 displayed significantly higher keratinocyte migration rates than the comparison groups [120]. This increase in cell migration was also observed in murine fibroblasts treated with rhEGF-loaded linoleic acid (LA)-CMCSNPs. Initially after 6 h of incubation, the increase

was significantly higher than untreated cells, and only slightly higher than cells treated with rhEGF alone [169]. However, at 12 h incubation, the rhEGF-loaded LA-CMCSNP group produced an evidently higher rate of cell migration than the rhEGF group [169]. The same study also showed that treatment with rhEGF-loaded LA-CMCSNPs led to a statistically significant increase in fibroblast cell proliferation [169].

7.7.3. *CS-modified metal NPs*

Although not immediately involved in the physical closure of wounds, the migration of macrophages is imperative in facilitating the wound healing process. Macrophages have a crucial role in the inflammatory phase which serves to stimulate other processes. Parthasarathy et al. reported improved murine macrophage cell migration rates in RAW 264.7 cells following treatment with CS-AgNPs [136]. Interestingly, the amount of cell migration observed at the study end-point of 48 h was similar for both CS-AgNPs (85%) and CS alone (82%) [136]. However, at the mid-point of 24 h, CS-AgNPs (73%) did have a notably higher cell migration rate than CS alone (56%) [136]. Both these groups had much higher migration rates than the $AgNO_3$ group which only had 38% and 59% scratch wound closure by 24 h and 48 h, respectively [136]. As seen in the results from this study, the modification of AgNPs with CS granted significant improvements in biological activity, in terms of promoting macrophage cell migration. Similarly, usage of CS in combination with AgNPs also served to improve the biological activity of CS in comparison to being used on its own.

7.8. *In vivo wound closure rate acceleration*

7.8.1. *CSNPs*

Numerous studies have attempted to assess the ability of CSNPs along with a wide range of therapeutic compounds to accelerate the wound healing process using animal models (Table 5). CSNP-encapsulated treatments and CS-modified metal NPs have been shown to reduce the time to achieve at least 80% wound closure from 5 or 7 d to 3–4 d in comparison to untreated wounds (Table 5). In complicated wound models such as diabetic wounds, the difference in healing rate in terms of time taken to achieve a high extent of wound closure may be difficult to compare as some of these wounds have delayed healing rates which extend beyond the study duration. This was also observed for some of the studies involving healthy animals due to the size of the wound or duration of the study. For cases such as these, the significant effects of the treatment groups can be observed in terms of the percentage of wound closure observed at the endpoint of the study (Table 6).

Along with measurements of the physical wound closure, studies have also reported histological observations of cross-sectional layers of the wound tissues using Haematoxylin and Eosin (H&E) and Masson's Trichrome (MT) staining. One study was conducted using CSNP-loaded calcium alginate hydrogels which showed significant improvements in the histological changes of healthy wound tissues throughout the treatment duration besides faster healing times [75]. This study showed that wound treatment with CSNPs facilitated faster resolution of wound inflammation with lower amounts of immune cell infiltration observed at earlier times than control wounds [75]. Higher degrees of granulation tissue formation, re-epithelialisation, and blood vessel maturation was also a prominent feature in wounds treated with CSNPs incorporated into hydrogels [75]. This phenomenon was also common among studies involving therapeutic agents encapsulated using CSNPs.

A significant observation reported in a study using epigallocatechin gallate (EGCG)-loaded CSNPs as a treatment in a diabetic wound model was the substantial decline in inflammatory cells present on Day 10 of treatment [170]. Although the wounds treated with CSNPs and EGCG showed statistically lower amounts of inflammatory cells around the wound bed, a more pronounced decrease was obtained when used in combination as EGCG-loaded CSNPs [170]. In contrast, Lopes Rocha Correa et al. had shown that treatment of diabetic wounds using MEL and CSNPs alone led to a similar suppression in polymorphonuclear leukocytes (PMNL) numbers on days 3 and 5 of treatment, respectively [166]. Surprisingly, this was not reflected in either day for MEL-loaded CSNP treatment groups [166]. Instead, only a modest decrease in PMNLs was observed in the wounds treated with MEL-loaded CSNPs on the same days where a sharp decline in PMNLs was reported for the 2 separate components [166]. The authors attributed this observation to the immediate exposure to MEL when free MEL was used as a treatment, in contrast to a slower exposure to MEL which have been encapsulated in CSNPs [166]. This enabled greater amounts of MEL to exhibit a larger antioxidative effect to suppress the inflammatory response [166]. However, the overall positive effects of encapsulating MEL in CSNPs in this study were credited to their ability to reduce its propensity to oxidation, which subsequently increased its half-life [166].

7.8.2. *CS-based nanogel*

Another study had developed alginate-coated CS nanogels carrying SSD specifically for burn wounds [171]. In their study, the authors reported that SSD-loaded alginate-coated CS nanogels produce significantly higher wound closure at both Day 5 and 10 when compared to both the control group and positive control group (marketed formulation of SSD) [171]. Interestingly, the developed nanogel contained 0.414% SSD of which rats were treated with 1% of the nanogel, whereas the positive control had a total SSD concentration of 0.1% [171]. Thus, the authors highlighted that SSD-loaded alginate-coated CS nanogels were able to produce faster wound healing speeds *in vivo* while using a lower concentration of SSD than the marketed formulation [171].

7.8.3. *CS-based NP complex*

NP complexes designed using COS and CUR^{3-} were evaluated as a potential wound healing tool in one study [102]. Generally, CUR-COS NP complexes were found to have faster wound closure rates and wound healing efficacy than CUR alone when used at the same dose of CUR [102]. Authors of this study proposed two primary factors which significantly contributed to the improved wound healing activity observed [102]. Firstly, the CUR-COS NP complexes were able to

Table 5 – Summary of studies evaluating the effects of CS-based NPs, CMCSNPs, CNPs, and CS-modified metal NPs on the wound closure rate in animal models in terms of the time taken to achieve almost complete wound closure.

NP formulation	Active ingredient	Encapsulation efficiency	Diameter	Surface charge	Wound Model (Animal Model)	Initial Wound Size	Time Taken to Achieve >80% Wound Closure	Ref.
Blank CS-based NPs								
CSNP[a]	–	–	77nm[†]	> +30mV	Diabetic pressure ulcer (Male Sprague-Dawley rat)	15 mm diameter	• Control (>21 d) • Oregano + Turmeric + CSNP ointment (15 d) • Oregano + Turmeric + CSNP hydrogel (>21 d) • Oregano + Turmeric + CSNP nanofibre (15 d)	[112]
CSNP[a]	–	–	208.40 ± 15.70 nm[†]	+24.20 ± 3.90 mV	Full-thickness wound (Female Sprague-Dawley rat)	20 mm diameter	• Control (>14 d) • CS-calcium alginate hydrogel (9 d) • CSNP-loaded calcium alginate hydrogel (7 d)	[75]
Therapeutic compound loaded CS-based NPs								
CSNP[f]	CDX	84.25% ± 0.02%	408.30 ± 53.17 nm[†]	+22.80 ± 0.57 mV	S. aureus infected full-thickness wound (Male albino rat)	5 mm diameter	• Control (>5 d) • CDX *in situ* gel (>5 d) • CDX-loaded CSNP *in situ* gel (5 d)	[118]
Alginate-coated CS nanogel[a]	SSD	41.34 ±%	697.19 nm[†]	−29.92 mV	Burn wound (Female rat)	–	• Control (> 10 d) • SSD-loaded alginate-coated CS nanogels (> 10 d)	[171]
CSNP[a]	QUE	90.00% ± 3.30%	361.16 ± 9.72 nm[†]	–	Full-thickness wound (Male Wistar rat)	≈400 mm^2	• Control (14 d) • QUE (14 d) • CSNP (14 d) • QUE-loaded CSNP (14 d)	[150]
CSNP[a]	VAC	51.70% ± 1.70%	216.60 ± 10.10 nm[†]	+37.10 ± 1.20 mV	Full-thickness wound (Sprague-Dawley rat)	10 mm diameter	• Control (10 d) • VAC (7 d) • CSNP (7 d) • VAC-loaded CSNP (7 d)	[149]
CSNP[a]	GA	73.20% ± 2.10%	252.90 ± 3.09 nm[†]	+33.50 ± 0.30 mV	Excision wound (Male Wistar rat)	2.0 × 2.0 cm^2	• Control (>16 d) • Collagen-fibrin scaffold containing GA-loaded CSNP (12 d)	[143]
CSNP[a]	CUR	–	196.40 nm[†]	+30.30 mV	Diabetic wound (Male Wistar rat)	2.0 × 2.0 cm^2	• Control (>15 d) • Collagen-alginate scaffold containing CUR-loaded CSNP (15 d)	[173]
CSNP[a]	CUR	77.20%	91.28 ± 4.30 nm[†]	–	Diabetic wound (Sprague-Dawley rat)	20 mm diameter	• Control (14 d) • CUR-loaded CSNP (7 d)	[148]
Gelatin/CSNP[c]	EGCG	45.80 ± 3.70%	236.60 ± 7.80 nm[†]	+28.90 ± 1.20 mV	S. aureus, E. coli, P. aeruginosa infected full-thickness wound (Male Sprague-Dawley rat)	1.0 × 1.0 cm^2	• Control (>12 d) • EGCG-loaded gelatin/CSNP + Activated carbon with gentamicin + γ-PGA/gelatin hydrogel (12 d)	[129]
CS/γ-PGA/pluronic/ CUR NP[h]	CUR	52.80 ± 4.70%	193.10 ± 8.90 nm[†]	+20.60 ± 2.40 mV	Full-thickness wound (Male Sprague-Dawley rat)	1.0 × 1.0 cm^2	• Control (12 d) • CS dressing (12 d) • CUR-loaded CS dressing (12 d) • CS dressing containing CS/γ-PGA/pluronic/ CUR NP (9 d)	[94]
CS-lecithin micelles[g]	TQ	98.77%	63.76 ± 14.78 nm[†]	–	Full-thickness wound (Balb/c mice)	1.0 × 1.0 cm^2	• Control (>16 d) • TQ (16 d) • TQ-loaded CS-lecithin micelles (12 d) • TQ-loaded CS-lecithin micelle hydrogel (12 d)	[172]

(*continued on next page*)

Table 5 (*continued*)

NP formulation	Active ingredient	Encapsulation efficiency	Diameter	Surface charge	Wound Model (Animal Model)	Initial Wound Size	Time Taken to Achieve >80% Wound Closure	Ref.
CUR-COS nanoplex[i]	CUR	–	140 ± 7 nm[†]	–	Full-thickness wound (Male mice)	8 mm diameter	• Control (7 d) • CUR (7 d) • CUR-COS nanoplex (5 d)	[102]
CSNP[a]	CUR	91.97%	257.70 ± 2.14 nm[†]	+30 ± 14 mV	Full-thickness wound (Male Wistar rat)	≈500 mm^2	• Control (>21 d) • CUR (21 d) • CSNP (>21 d) • CUR-loaded CSNP (21 d)	[174]
Gelatin/CSNP[c]	EGCG & Ascorbic acid	68.39 ± 2.60%	286.78 ± 3.02 nm[†]	+29.90 ± 0.59 mV	Diabetic full-thickness wound (Male ICR mice)	6 mm diameter	• Control (>10 d) • EGCG (10 d) • CSNP (10 ds) • EGCG-loaded gelatin/CSNP (8 d)	[170]
CSNP[a]	CUR	93.00 ± 5.00%	359 ± 65 nm[†]	−10.70 ± 0.10 mV	Full-thickness wound (Male Wistar rat)	1.5 × 1.5 cm^2	• Control (>14 d) • CSNP-loaded PCL-gelatin nanofibre (>14 d) • CUR-loaded CSNP (>14 d) • PCL-gelatin nanofibre containing CUR-loaded CSNP (14 d)	[156]
CSNP[a]	Insulin	77%	294.50 ± 21.92 nm[†]	+17.89 ± 0.74 mV	Full-thickness wound (Male Wistar rat)	1.5 × 1.5 cm^2	• Control (>14 d) • PCL-collagen scaffold containing insulin-loaded CSNP (14 d)	[130]
CSNP[a]	GM-CSF	97.40 ± 1.68%	366.90 ± 9.15 nm[†]	+43.52 ± 2.39 mV	Full-thickness wound (Male Wistar rat)	1.5 × 1.5 cm^2	• Control (>13 d) • CSNP-loaded cellulose nanocrystal-hyaluronic acid composite (8 d) • Cellulose nanocrystal-hyaluronic acid composite containing GM-CSF-loaded CSNP (8 d)	[175]
Lecithin/CSNP[g]	MEL	27%	160.43 ± 4.45 nm[†]	+25.00 ± 0.57 mV	Diabetic full-thickness wound (Wistar rat)	9 mm diameter	• Control (>14 d) • MEL (>14 d) • Lecithin/CSNP (14 d) • MEL-loaded lecithin/CSNP (14 days)	[166]
CSNP[a]	Insulin	97.19% ± 2.18%	245.90 ± 25.46 nm[†]	+39.30 ± 4.88 mV	Diabetic full-thickness wound (Female Wistar rat)	8 mm diameter	• Insulin (>14 d) • CSNP (>14 d) • Insulin-loaded CSNP (>14 d)	[176]
CSNP[a]	GM-CSF	80.15% ± 0.56%	400 nm[†]	–	Full-thickness wound (Male Wistar rat)	20 mm diameter	• Control (16 d) • CSNP-loaded PCL scaffold (14 d) • PCL scaffold containing (G-CSF)-loaded CSNP (12 d)	[177]
CMCSNPs								
CMCSNP[d]	OH30	82.46% ± 1.11%	258.70 ± 13.30 nm[†]	+30.20 ± 5.10 mV	Full-thickness wound (Female Kunming mice)	7 mm diameter	• Control (15 d) • OH30 (15 d) • CMCSNP (15 d) • OH30-loaded CMCSNP (10 d)	[120]
Conjugated LA-CMCSNP[g]	rhEGF	82.43% ± 3.14%	155.30 ± 4.62 nm[†]	−23.30 ± 0.37 mV	Full-thickness wound (Rat)	2.54 cm^2	• Control (14 d) • rhEGF (11 d) • LA-CMCSNP (14 d) • rhEGF-loaded LA-CMCSNP (7 d)	[169]

(*continued on next page*)

Table 5 (*continued*)

NP formulation	Active ingredient	Encapsulation efficiency	Diameter	Surface charge	Wound Model (Animal Model)	Initial Wound Size	Time Taken to Achieve >80% Wound Closure	Ref.
CMCSNP[e]	OH30	92.14% ± 1.05%	164.60 ± 5.00 nm[†]	−37.60 ± 1.50 mV	Full-thickness wound (Female Kunming mice)	7 mm diameter	• Control (12 d) • CMCSNP (9 d) • OH30-loaded CMCSNP (6 d)	[121]
CNPs								
CNP[g]	–	–	14 ± 3 nm[§]	–	Full-thickness wound (Male Sprague-Dawley rat)	10 mm diameter	• Control (>9 d) • CNP Cryogel (9 d) • CNP Aerogel (>9 d)	[158]
CS-modified metal NPs								
CS-modified ZnONP[‖]	ZnO	–	~180 nm[¶]	–	Full-thickness wound (Sprague-Dawley rat)	1.5 × 1.5 cm^2	• Control (>14 d) • CS-ZnONP-loaded CO film (10 d)	[131]
CS-AgNP[#]	Ag	–	5 – 50 nm[§]	–	Full-thickness wound (Male Kunming mice)	10 mm diameter	• Control (>14 d) • CS-Bletilla striata (BG) sponge (14 d) • CS-BG + CS-AgNP bilayer sponge (14 d)	[132]
PVA/CS-AgNP[#]	Ag	–	190 – 200 nm[†,§]	–	Full-thickness wound (Male Wistar rat)	1.5 × 1.0 cm^2	• Control (12 d) • CS (10 d) • CS-PVA (10 d) • PVA/CS-AgNP (9 d)	[134]
COS-AgNP[#]	Ag	–	15.70 ± 4.73 nm[§]	–	Full-thickness wound (Sprague-Dawley rat)	5.0 × 4.0 cm^2	• Control (12 d) • PVA/COS/$AgNO_3$ nanofibre • PVA/COS-AgNP nanofibre (7 d)	[123]
PVA/COS-AgNP[#]	Ag	–	–	–	Full-thickness wound (Male Sprague-Dawley rat)	≈200 mm^2	• Control (15 d) • PVA/COS-AgNP nanofibre (12 d)	[159]
MMT-CS-AuNP[#]	Au	–	10.07 ± 2.34 nm[†]	–	MRSA infected full-thickness wounds (New Zealand rabbits)	25 mm diameter	• Control (>16 d) • CS-AuNP-loaded gelatin (16 d) • MMT-CS-AuNP-loaded gelatin (16 d)	[135]
CS-AgNP[#]	Ag	–	15 nm[§]	–	Burn wound (Male Sprague-Dawley rat)	10 mm diameter	• Control (14 d) • CS-AgNP (7 d)	[141]
CS-AgNP[#]	Ag	–	22.80 nm[†]	−45.90 Mv (DLS)	Abrasion wound (Male Wistar rat)	1.5 × 1.5 cm^2	• Control (21 d) • CS film (21 d) • CS-AgNP-loaded CS film (5 d)	[124]
CS-AgNP[#]	Ag	–	10 - 30 nm[§]	–	MRSA infected full-thickness wound (Balb/c mice)	1.5 × 1.5 cm^2	• Control (14 d) • AgNP (10 d) • PVP-AgNP (10 ds) • CS-AgNP (10 d)	[137]
CS-SER-AgNP[#]	Ag	–	96.93 ± 0.51 nm[†]	−0.42 ± 0.12mV	S. aureus infected burn wound (Male Sprague-Dawley rat)	≈400 mm^2	• Moxifloxacin (>14 d) • CS-SER-AgNP film (7 d)	[138]
CS-SER-AgNP[#]	Ag	–	96.93 ± 0.51 nm[†]	−0.42 ± 0.12mV	P. aeruginosa infected burn wound (Male Sprague-Dawley rat)	≈400 mm^2	• Moxifloxacin (>14 d) • CS-SER-AgNP film (14 d)	[138]

(*continued on next page*)

Table 5 (*continued*)

NP formulation	Active ingredient	Encapsulation efficiency	Diameter	Surface charge	Wound Model (Animal Model)	Initial Wound Size	Time Taken to Achieve >80% Wound Closure	Ref.
CS-SER-AgNP[#]	Ag	–	239.90 ± 1.56 nm[†]	+37.00 ± 3.60 mV	Full-thickness wound (Wistar rat)	10 mm diameter	• Control (>14 d) • CS-SER-AgNP (>14 d)	[139]
TMC-immobilised AgNP[‡]	Ag	–	–	–	Full-thickness wound (Mice)	–	• Control (>7 d) • CS (>7 d) • TMC (>7 d) • TMC-AgNP (>7 d)	[110]

[f] Prepared using W/O/W type double emulsification.
[g] Prepared using self-assembly.
[h] Prepared using emulsification solvent diffusion method and homogenisation.
[i] Prepared using polyelectrolyte complex method.
[‖] Prepared using precipitation method.
[#] Prepared using chemical reduction method.
[‡] Prepared using template method.
[†] Size measured using DLS.
[¶] Size measured using SEM.
[§] Size measured using TEM

produce a higher concentration of CUR at the wound site compared to applying CUR to the wound site on its own [102]. Secondly, the additional biological activity of COS when used in combination with CUR further increased the overall efficacy. Histological examination revealed that both CUR-COS NP complex and CUR treatment groups had higher collagen deposition than the control group [102]. The authors also reported the CUR-COS NP complex group to have the smallest amount of scar tissue present among all [102].

7.8.4. *CS-based polymeric micelle*

A study using thymoquinone (TQ)-loaded lecithin-CS polymeric micelles incorporated into hydrogels had showed improved rates of tissue maturation at the study end-point, including the appearance of thicker epidermal layers, an organised layer of collagen fibre, increased quantities of fibroblasts and new vessels, along with the scarcity of inflammatory cells when compared to untreated wounds and positive control wounds treated with SSD [172]. Improvements were still observed in wounds treated with the therapeutic agent, TQ alone, where reduced inflammatory cells and increased collagen formation was seen [172]. However, this observation was much more pronounced in the wounds treated with TQ loaded into lecithin-CS polymeric micelles [172].

A variety of different NPs other than the conventional CSNPs can be seen to be effective in designing potential pharmaceutical formulations in treating different wounds. These studies demonstrated that using NPs in the form of nanogels, NP complexes, and polymeric micelles can produce enhanced therapeutic outcomes.

7.8.5. *CMCSNPs*

When studying the positively charged OH30-loaded CS-coated CMCSNPs, microscopic evaluation of wound tissues revealed more intricate improvements accompanying the accelerated wound healing rate [120]. At the study end-point of 15 days, wounds treated with OH30-loaded CS-coated CMCSNPs had a visibly thicker and more robust re-epithelialisation layer than all the other groups [120]. Authors of this study also found that CS-coated CMCSNPs allowed OH30 to permeate deeper into the skin of nude mice and can be retained for a much longer time as compared to OH30 alone [120]. This may be a significant contributing factor which allowed the developed formulation to produce wound regeneration at higher speeds and higher quality than when using OH30 alone [120].

Another study which evaluated negatively charged OH30-loaded CMCSNPs also found both faster healing speeds and better wound healing quality following treatment with their formulation [121]. Zou et al. found that treatment with OH30-loaded CMCSNPs not only reduced the time taken for wound closure but also observed significant changes histologically [121]. The wounds treated with OH30-loaded CMCSNPs had accelerated re-epithelialisation and collagen deposition which were considered to be a factor in the faster wound healing observed by the authors [121]. Although the two studies using both OH30 and CMCSNPs had major differences in overall particle surface charge, the wound healing effects of both components were still retained [120,121]. To gain more insight on this, future studies on negatively charged OH30-loaded CMCSNPs could be prompted to evaluate the distribution of OH30 in skin and the retention time of the compound to compare this aspect with positively charged OH30-loaded CS-loaded CMCSNPs.

Conjugated LA-CMCSNPs carrying rhEGF were also successfully formulated to improve wound healing in animals [169]. The rhEGF-loaded LA-CMCSNPs were able to produce faster wound closure than blank LA-CMCSNPs and rhEGF alone [169]. All three treatment groups had faster wound closure than the control group [169]. H&E staining further revealed more complete regeneration of

Table 6 – Summary of studies evaluating the effects of CS-based NPs and CS-modified metal NPs on the wound closure rate in animal models in terms of the percentage wound closure at the study end-point.

NP formulation	Active ingredient	Encapsulation efficiency	Diameter	Surface charge	Wound Model (Animal Model)	Initial Wound Size	Percentage Wound Closure at Study End-point	Ref.
Therapeutic compound loaded CS-based NPs								
Alginate-coated CS nanogel[a]	SSD	41.35%	697.19 nm[†]	−29.92 mV	Burn wound (Female rat)	–	• Control (16.07% ± 1.52%) • SSD (34.53 ± 2.61%) • SSD-loaded alginate-coated CS nanogel (49.61% ± 5.01%)	[171]
CSNP[a]	QUE	90.00% ± 3.30%	361.16 ± 9.72 nm[†]	–	Full-thickness wound (Male Wistar rat)	≈400 mm^2	• Control (>90%) • QUE (>90%) • CSNP (>90%) • QUE-loaded CSNP (>90%)	[150]
CSNP[a]	CUR	–	196.40 nm[†]	+30.30 mV	Diabetic wound (Male Wistar rat)	2.0 × 2.0 cm^2	• Control (44.6% ± 6.3%) • Collagen-alginate scaffold containing • CUR-loaded CSNP (98.1% ± 3.4%)	[173]
Gelatin/ CSNP[c]	EGCG	45.80% ± 3.70%	236.60 ± 7.80 nm[†]	+28.90 ± 1.20 mV	S. aureus, E. coli, P. aeruginosa infected full-thickness wound (Male Sprague-Dawley rat)	1.0 × 1.0 cm^2	• Control (≈70%) • EGCG-loaded gelatin/CSNP + Activated carbon with gentamicin + γ-PGA/gelatin hydrogel (≈90%)	[129]
CSNP[a]	CUR	91.97%	257.70 ± 2.14 nm[†]	+30 ± 14mV	Full-thickness wound (Male Wistar rat)	≈500 mm^2	• Control (≈20%) • CUR (≈90%) • CSNP (≈65%) • CUR-loaded CSNP (≈100%)	[174]
CSNP[a]	CUR	93.00% ± 5.00%	359 ± 65 nm[†]	−10.70 ± 0.10 mV	Full-thickness wound (Male Wistar rat)	1.5 × 1.5 cm^2	• Control (42.5% ± 4.7%) • CSNP-loaded PCL-gelatin nanofibre (≈65%) • CUR-loaded CSNP (73.4% ± 3.2%) • PCL-gelatin nanofibre containing CUR-loaded CSNP (82%)	[156]
CSNP[a]	Insulin	77%	294.50 ± 21.92 nm[†]	+17.89 ± 0.74 mV	Full-thickness wound (Male Wistar rat)	1.5 × 1.5 cm^2	• Control (45.70% ± 4.06%) • PCL-collagen scaffold containing insulin-loaded CSNP (96.90 ± 1.11%)	[130]
Lecithin/ CSNP[g]	MEL	27%	160.43 ± 4.45 nm[†]	25.00 ± 0.57mV	Diabetic full-thickness wound (Wistar rat)	9 mm diameter	• Control (≈27%) • MEL (≈13%) • Lecithin/CSNP (≈40%) • MEL-loaded lecithin/CSNP (≈44%)	[166]
CSNP[a]	Insulin	97.19% ± 2.18%	245.90 ± 25.46 nm[†]	+39.30 ± 4.88 mV	Diabetic full-thickness wound (Female Wistar rat)	8 mm diameter	• Insulin (≈100%) • CSNP (≈100%) • Insulin-loaded CSNP (≈100%)	[176]
CS-modified metal NPs								
CS-AgNP[#]	Silver, Ag	–	5 – 50 nm[§]	–	Full-thickness wound (Male Kunming mice)	10 mm diameter	• Control (76.35%) • CS-BG sponge (87.7%) • CS-BG + CS-AgNP bilayer sponge (89.3%)	[132]
MMT-CS-AuNp[#]	Gold, Au	–	10.07 ± 2.34 nm[†]	–	MRSA infected full-thickness wounds (New Zealand rabbits)	25 mm diameter	• Control (67%) • CS-AuNP loaded gelatin (83%) • MMT-CS-AuNP-loaded gelatin (91.5%)	[135]
CS-SER-AgNP[#]	Silver, Ag	–	239.90 ± 1.56 nm[†]	+37.00 ± 3.60 mV	Full-thickness wound (Wistar rat)	10 mm diameter	• Control (40% ± 3.92%) • CS-SER-AgNP (70% ± 3.14%)	[139]

(*continued on next page*)

Table 6 (*continued*)

NP formulation	Active ingredient	Encapsulation efficiency	Diameter	Surface charge	Wound Model (Animal Model)	Initial Wound Size	Percentage Wound Closure at Study End-point	Ref.
TMC-immobilised AgNP[‡]	Silver, Ag	–	–	–	Full-thickness wound (Mice)	–	• Control (≈45%) • CS (≈60%) • TMC (≈60%) • TMC-immobilised AgNP (≈70%)	[110]

[a] Prepared using ionic gelation method with TPP as a cross-linker.
[c] Prepared by gelation of CS and gelatin mixture.
[g] Prepared using self-assembly.
[#] Prepared using chemical reduction method.
[‡] Prepared using template method.
[†] Size measured using DLS.
[§] Size measured.

the underlying skin tissue in wounds treated by the rhEGF-loaded LA-CMCSNPs [169]. A thicker epidermis along with an increase in epidermal cells, fibroblasts, and collagen was seen [169]. Hence, the applicability of CMCSNPs in wound healing is not limited to unmodified CMCSNPs alone. Positive outcomes are able to be achieved by designing NP carriers using CMCS conjugates such as LA-CMCSNPs in this study [169].

7.8.6. CNPs

CNPs formulated into both cryogels and aerogels exhibited faster wound closure than both the control (gauze) and positive control (DuoDERM®) [158]. The group treated with CNP aerogels had smaller wound areas than the cryogels throughout the study duration except at the end-point where the cryogels had a smaller final wound area than aerogels [158]. Both the CNP aerogels and cryogels produced lesser inflammatory cells by Day 7 and more fibroblast cells by Day 14 based on histological analysis [158]. However, the CNP aerogels had the formation of more matured blood vessels and epithelial layer than the other groups [158]. By using CD31 immunostaining, the authors also found that the matured blood vessels of the CNP aerogel group were larger on Day 7 and were smallest by Day 14 [158]. Histological analysis further revealed increased collagen deposition and improved alignment in CNP aerogel groups [158]. Overall, the results suggested that CNPs in the form of aerogels may hold better promise in improving wound healing outcomes than CNPs in the form of cryogels [158]. However, both designs using CNPs as the base have been found to significantly improve wound healing [158].

7.8.7. CS-modified metal NPs

Wound tissues treated with castor oil (CO) films loaded with CS-ZnONPs had noticeably less inflammatory markers at the study end-point along with denser, more compact, and better aligned collagen fibres than wounds treated with blank CO films [131]. To show the added benefits of modifying AgNPs with COS, a study examined the different results obtained using PVA/COS-AgNP against PVA/COS/$AgNO_3$ [123]. Once again, the PVA/COS-AgNP showed superior wound healing with improved granulation tissue maturation, re-epithelialisation, and vessel formation than the PVA/COS/$AgNO_3$ treatment group [123].

In terms of infected burn wounds, Shah et al. showed that film dressings developed using CS-sericin (SER)-AgNPs had significantly improved wound healing abilities than treatment with moxifloxacin alone [138]. This effect was slightly higher in S. aureus infected wounds than P. aeruginosa infected wounds [138]. Histological results illustrated that CS-SER-AgNP treatment groups had the highest degree of collagen formation, fastest resolution of wound inflammation, and improved angiogenesis rate than the positive control group treated with commercial Bactigras® [138]. The strong antibacterial nature of the formulated CS-SER-AgNPs was thought to be the primary factor contributing to this positive outcome [138].

A preclinical study on the treatment of MRSA-infected wounds using CS-AgNPs by Peng et al. had also produced encouraging results [137]. In terms of wound healing speed, CS-AgNPs had very similar results to those of uncoated-AgNPs and polyvinylpyrrolidone (PVP)-AgNPs [137]. However, coating AgNPs in the form of CS-AgNPs greatly reduced the amount of silver detected on newly healed skin tissue by almost half as compared to uncoated-AgNPs and PVP-AgNPs [137]. Similarly, treatment with CS-AgNPs was found to have a significant impact on silver content detected in the liver [137]. Topically applied CS-AgNPs produced a much lower deposition on silver in the liver as compared to uncoated-AgNPs and PVP-AgNPs administered in the same manner [137]. The findings from this study provide an additional angle supporting the usage of CS in modifying metal NPs. Although enhancement in bioactivity may not necessarily be achieved by modifying AgNPs with CS, other aspects such as safety and distribution can be significantly improved.

8. Future prospects

The end goals in the development of wound dressings are to improve patient healthcare and wound healing outcomes [6,8]. In order to achieve this purpose, there is a need for a strong database of evidence supporting the overall clinical and therapeutic functionality of wound dressings in development.

Emerging novel and innovative nanoformulations for wound care applications have expanded the number of options and possibilities in designing modern wound dressings. Studies investigating nanoformulations such as NP-based systems for dermal wound healing often take advantage of the smaller particle sizes for better skin penetration and controlled delivery of active compounds [71]. Despite this fact, there are limited studies that report on the degree of skin penetration of the investigated active compound against the active compound embedded within the CS-based NP formulation [178]. As certain active compounds exhibit poor skin penetration or short half-lives, data demonstrating the usage of CS-based NPs to overcome this weakness is valuable to the scientific community. The notable rise in amount of research focusing on the development of nanoformulations for wound healing purposes has been astonishing over the past few years [58-60,71]. Search results for the terms "Nanoparticle" AND "Wound Healing" on PubMed has increased by about 10 times from the year 2010 with 41 results to 2020 with 443 results. Development of nanoformulations within this field has shown enormous potential for improving patient outcomes [58-60,71]. Functional properties ranging from microbial inhibition to directly stimulating tissue regeneration have been thoroughly explored using these nanoformulations [179,180]. This widely diverse set of applications have been made possible due to the nature of nanomaterials as a platform which enables the usage of various active agents; some of which become less feasible without the use of these nanoformulations [179,180]. These agents include but are not limited to proteins, peptides, growth factors, and stem cells [179,180]. Necessary actions involving funding and future investments must be carefully taken to ensure the continuity of research in this area to capitalise on the maximum potential of nanotechnology and improve our understanding of this modern tool.

On another note, there are large numbers of studies providing substantial amounts of information regarding the antibacterial effects of CS-based NPs and CS-modified metal NPs, particularly involving the combination with active compounds, such as CUR and AgNPs. However, there are limited studies investigating the inhibitory effects of these formulations on bacterial biofilm in wound healing, despite documented evidence of CS's anti-biofilm properties [181–183]. Another gap identified in the literature is that most of the studies involving CS-modified metal NPs are conducted on normal healthy wounds or infected wounds. It would be interesting to expand the potential of these CS-modified metal NPs into more complicated types of wounds, such as diabetic wounds, which will bring a whole new perspective to chronic wound management. Furthermore, a deep understanding on the mechanistic actions of CS-based NPs in terms of their wound healing effects is necessary in order to optimise their use and understand the possible interactions that may arise when used in combination with other products.

Although a number of studies discussed in this literature review included the use of CS derivatives such as CMCS, the total number of studies examining these derivatives in the form of NPs for wound healing are relatively low [120,121,169]. It could be seen that CS-coated CMCSNPs could potentially provide better performance for certain aspects such as antimicrobial activity than CMCSNPs, however, more studies will be required before an adequate comparison can be made with CS-based NPs and other derivatives [120]. It was also noticed that CMCSNPs were more commonly used in combination with OH30, which was less commonly used together with CS-based NPs among the wound healing studies [120,121]. This may be due to the cationic nature of OH30 which allows them to form NPs more easily with the negatively charged CMCS rather than positively charged CS.

Usage of CS-based nanogels, NP complexes, and polymeric micelles have also been under-represented in the current literature. Although, promising results have been produced by studies evaluating these nanoformulations, the minimal amount of studies available greatly limits any discussion on their applicability. It would be interesting to see the comparison of wound healing efficacy between these nanoformulations and CSNPs.

There have been a number of clinical trials conducted on CS-based wound dressings in various settings including normal open wounds, diabetic foot ulcers, burns, and surgical wounds [184,185]. However, to our best knowledge, there has been a distinct lack of studies involving the use of CS-based NPs in the form of a wound dressing in a clinical trial setting. There is already a wealth of pre-clinical animal studies consisting of a wide range of both animal models and wound types which can provide the necessary knowledge to begin the venture into clinical models in a suitable setting. Recognizing the underlying healthcare burdens of wounds in the clinical setting, the development of a revolutionary wound healing dressing will provide substantial relief to both clinicians and patients. Indeed, great strides have been made in terms of wound dressings used across the past decades, from traditional cotton gauzes to synthetic polymer-based dressings with bioactive components. Further incorporation of newer cutting-edge technologies such as NP systems in developing the next generation of wound dressings is crucial in improving wound management within the healthcare industry. The progression from *in vitro* cell cultures and *in vivo* animal models into clinical trials is an imperative step in determining the feasibility and impact of applying CS-based NPs in this field of medicine.

Additionally, despite the strong evidence supporting the benefits of using CS-based NPs, they are not without certain drawbacks or limitations. Firstly, the poor solubility of CS in neutral and alkaline solutions limit its widespread use as CS-based NPs [186,187]. High variability in polymer properties which lead to large variations in biological activity of the final product also causes difficulty in standardisation [186,187]. Although, many studies advocated the biodegradability of CS, a large portion of these studies only quote the biodegradability

of the polymer without investigating the final CS-based formulation [188]. This is even more prominent in studies using CS-based NPs. More research on the biodegradability of CS-based NPs and their impact on the environment is necessary before its use can be widely accepted [188]. Due to the antimicrobial nature of CS, there is also a need to understand the impact of CS-based NPs on the environmental microbiome upon their disposal [189]. Numerous studies have evaluated the toxicity and biocompatibility of CS-based NPs within the context of their application. However, there is a need for studies investigating the full potential toxicity profile of CS-based NPs to ensure safe and efficacious usage [190]. Furthermore, there is also a greater challenge in scaling up the preparation of CS-based NPs for mass-production as compared to CS-based materials in general [191].

9. Conclusion

By taking advantage of the known biological properties of CS, researchers have seized the opportunity to study its application in treating wounds and skin tissue injury in the form of various types of formulations, ranging from hydrogels and aerogels to film membranes and nanofibres. CS-based NPs are only a small subset of this large family of wound dressings with CS as its common factor. Designing CS-based wound dressings in the form of NPs provides the additional advantage of having better tissue penetration and overall activity due to the smaller sizes and flexible surface structure. Another fascinating feature of this design is the added opportunity of transporting other therapeutic agents which can act in combination with the CS-based NPs. Acknowledging this fact, many studies have encapsulated actives such as natural compounds, peptides, and antibiotics using various forms of CS-based NPs when formulating a wound dressing. However, more research will be required to overcome the challenges associated with using CSNPs such as the limited of biodegradability data, its impact on the environment, and scalability.

Overall, the variety of different CS-based NPs, CMCSNPs, CNPs, and CS-modified metal NPs were shown to have promising wound healing effects from numerous perspectives such as wound haemostasis, microbial growth inhibition, anti-oxidation, inflammatory modulation, and angiogenetic regulation, among many others which cumulatively contribute to wound healing rate acceleration. Despite a small number of studies showing lack of expected outcome, majority of evidence have demonstrated superior wound healing effects by these formulations, either used on their own or as drug delivery vehicle to encapsulate wound healing agent. This is a testament to the remarkable versatility and applicability of these nanoformulation in developing wound healing treatments. Quality formulation design and rigorous optimisation are key to construct nanoformulations with desired properties, to further advance the field of drug delivery in the application of wound healing.

Conflicts of interesting

The authors report no conflicts of interest. The authors alone are responsible for the content and writing of this article.

Acknowledgements

This project was not supported by any financial support from grants provided by any funding agencies in public, commercial, or not-for-profit sectors. All the figures published in this article were produced using the Biorender.com application.

REFERENCES

[1] Martinengo L, Olsson M, Bajpai R, Soljak M, Upton Z, Schmidtchen A, et al. Prevalence of chronic wounds in the general population: systematic review and meta-analysis of observational studies. Ann Epidemiol 2019;29:8–15.
[2] Olsson M, Järbrink K, Divakar U, Bajpai R, Upton Z, Schmidtchen A, et al. The humanistic and economic burden of chronic wounds: a systematic review. Wound Repair Regen 2019;27(1):114–25.
[3] Guest JF, Fuller GW, Vowden P. Cohort study evaluating the burden of wounds to the UK's National Health Service in 2017/2018: update from 2012/2013. BMJ Open 2020;10(12):e045253.
[4] Yao Z, Niu J, Cheng B. Prevalence of chronic skin wounds and their risk factors in an inpatient hospital setting in northern China. Adv Skin Wound Care 2020;33(9).
[5] Lo ZJ, Lim X, Eng D, Car J, Hong Q, Yong E, et al. Clinical and economic burden of wound care in the tropics: a 5-year institutional population health review. Int Wound J 2020;17(3):790–803.
[6] Kus KJB, Ruiz ES. Wound dressings – a practical review. Curr Dermatol Rep 2020;9(4):298–308.
[7] Dhivya S, Padma VV, Santhini E. Wound dressings - a review. Biomedicine 2015;5(4):22–8.
[8] Rezvani Ghomi E, Khalili S, Nouri Khorasani S, Esmaeely Neisiany R, Ramakrishna S. Wound dressings: current advances and future directions. J Appl Polym Sci 2019;136(27):47738.
[9] Tottoli EM, Dorati R, Genta I, Chiesa E, Pisani S, Conti B. Skin wound healing process and new emerging technologies for skin wound care and regeneration. Pharmaceutics 2020;12(8):735.
[10] Rajendran NK, Kumar SSD, Houreld NN, Abrahamse H. A review on nanoparticle based treatment for wound healing. J Drug Deliv Sci Technol 2018;44:421–30.
[11] Rodrigues M, Kosaric N, Bonham CA, Gurtner GC. Wound healing: a cellular perspective. Physiol Rev 2018;99(1):665–706.
[12] Sorg H, Tilkorn DJ, Hager S, Hauser J, Mirastschijski U. Skin wound healing: an update on the current knowledge and concepts. Eur Surg Res 2017;58(1–2):81–94.
[13] Boer M, Duchnik E, Maleszka R, Marchlewicz M. Structural and biophysical characteristics of human skin in maintaining proper epidermal barrier function. Postepy Dermatol Alergol 2016;33(1):1–5.

[14] Gurtner GC, Werner S, Barrandon Y, Longaker MT. Wound repair and regeneration. Nature 2008;453(7193):314–21.
[15] Krzyszczyk P, Schloss R, Palmer A, Berthiaume F. The role of macrophages in acute and chronic wound healing and interventions to promote pro-wound healing phenotypes. Front Physiol 2018;9:419.
[16] Schäffer M, Barbul A. Lymphocyte function in wound healing and following injury. BJS (British Journal of Surgery) 1998;85(4):444–60.
[17] desJardins-Park HE, Foster DS, Longaker MT. Fibroblasts and wound healing: an update. Regen Med 2018;13(5):491–5.
[18] P B. Wound healing and the role of fibroblasts. J Wound Care 2013;22(8):407–12.
[19] Pastar I, Stojadinovic O, Yin NC, Ramirez H, Nusbaum AG, Sawaya A, et al. Epithelialization in wound healing: a comprehensive review. Adv Wound Care 2014;3(7):445–64.
[20] Cañedo-Dorantes L, Cañedo-Ayala M. Skin acute wound healing: a comprehensive review. Int J Inflam 2019;2019 3706315.
[21] Han G, Ceilley R. Chronic Wound healing: a review of current management and treatments. Adv Ther 2017;34(3):599–610.
[22] Frykberg RG, Banks J. Challenges in the treatment of chronic wounds. Adv Wound Care 2015;4(9):560–82.
[23] Muxika A, Etxabide A, Uranga J, Guerrero P, de la Caba K. Chitosan as a bioactive polymer: processing, properties and applications. Int J Biol Macromol 2017;105:1358–68.
[24] Zhao D, Yu S, Sun B, Gao S, Guo S, Zhao K. Biomedical applications of chitosan and its derivative nanoparticles. Polymers (Basel) 2018;10(4):462.
[25] Feng P, Luo Y, Ke C, Qiu H, Wang W, Zhu Y, et al. Chitosan-based functional materials for skin wound repair: mechanisms and applications. Front Bioeng Biotechnol 2021;9:111.
[26] Ali Khan Z, Jamil S, Akhtar A, Mustehsan Bashir M, Yar M. Chitosan based hybrid materials used for wound healing applications- A short review. International Journal of Polymeric Materials and Polymeric Biomaterials 2020;69(7):419–36.
[27] Patrulea V, Ostafe V, Borchard G, Jordan O. Chitosan as a starting material for wound healing applications. Eur J Pharm Biopharm 2015;97:417–26.
[28] Liu L, Gao Q, Lu X, Zhou H. In situ forming hydrogels based on chitosan for drug delivery and tissue regeneration. Asian J Pharmaceut Sci 2016;11(6):673–83.
[29] Sabab A, Vreugde S, Jukes A, Wormald PJ. The potential of chitosan-based haemostats for use in neurosurgical setting – Literature review. J Clin Neurosci 2021;94:128–34.
[30] Goy RC, Dd Britto, Assis OBG. A review of the antimicrobial activity of chitosan. Polímeros 2009;19:241–7.
[31] Kong M, Chen XG, Xing K, Park HJ. Antimicrobial properties of chitosan and mode of action: a state of the art review. Int J Food Microbiol 2010;144(1):51–63.
[32] Dunnill C, Patton T, Brennan J, Barrett J, Dryden M, Cooke J, et al. Reactive oxygen species (ROS) and wound healing: the functional role of ROS and emerging ROS-modulating technologies for augmentation of the healing process. Int Wound J 2017;14(1):89–96.
[33] Wlaschek M, Scharffetter-Kochanek K. Oxidative stress in chronic venous leg ulcers. Wound Repair Regen 2005;13(5):452–61.
[34] Ngo DH, Kim SK. Antioxidant effects of chitin, chitosan, and their derivatives. In: Kim SK, editor. Advances in food and nutrition research. Academic Press; 2014. p. 15–31.
[35] Si Trung T, Bao HND. Physicochemical properties and antioxidant activity of chitin and chitosan prepared from pacific white shrimp waste. International Journal of Carbohydrate Chemistry 2015;2015:706259.
[36] Demidova-Rice TN, Hamblin MR, Herman IM. Acute and impaired wound healing: pathophysiology and current methods for drug delivery, part 1: normal and chronic wounds: biology, causes, and approaches to care. Adv Skin Wound Care 2012;25(7):304–14.
[37] Fong D, Hoemann CD. Chitosan immunomodulatory properties: perspectives on the impact of structural properties and dosage. Future Sci OA 2017;4(1):FSO225.
[38] Hoemann CD, Fong D. 3 - Immunological responses to chitosan for biomedical applications. In: Jennings JA, Bumgardner JD, editors. Chitosan based biomaterials. Chitosan based biomaterials, 1. Woodhead Publishing; 2017. p. 45–79.
[39] Yang EJ, Kim JG, Kim JY, Kim S, Lee N, Hyun CG. Anti-inflammatory effect of chitosan oligosaccharides in RAW 264.7 cells. Open Life Sci 2010;5(1):95–102.
[40] Chang SH, Lin YY, Wu GJ, Huang CH, Tsai GJ. Effect of chitosan molecular weight on anti-inflammatory activity in the RAW 264.7 macrophage model. Int J Biol Macromol 2019;131:167–75.
[41] Wu N, Wen Z-S, Xiang XW, Huang YN, Gao Y, Qu YL. Immunostimulative activity of low molecular weight chitosans in RAW264.7 macrophages. Mar Drugs 2015;13(10).
[42] Zheng B, Wen ZS, Huang YJ, Xia MS, Xiang XW, Qu YL. Molecular weight-dependent immunostimulative activity of low molecular weight chitosan via regulating NF-κB and AP-1 signaling pathways in RAW264.7 macrophages. Mar Drugs 2016;14(9).
[43] Hattori H, Ishihara M. Changes in blood aggregation with differences in molecular weight and degree of deacetylation of chitosan. Biomedical Materials 2015;10(1): 015014.
[44] Yang J, Tian F, Wang Z, Wang Q, Zeng YJ, Chen SQ. Effect of chitosan molecular weight and deacetylation degree on hemostasis. J Biomed Mater Res Part B 2008;84B(1):131–7.
[45] Chang SH, Lin HTV, Wu GJ, Tsai GJ. pH Effects on solubility, zeta potential, and correlation between antibacterial activity and molecular weight of chitosan. Carbohydr Polym 2015;134:74–81.
[46] Mellegård H, Strand SP, Christensen BE, Granum PE, Hardy SP. Antibacterial activity of chemically defined chitosans: influence of molecular weight, degree of acetylation and test organism. Int J Food Microbiol 2011;148(1):48–54.
[47] No HK, Young Park N, Ho Lee S, Meyers SP. Antibacterial activity of chitosans and chitosan oligomers with different molecular weights. Int J Food Microbiol 2002;74(1):65–72.
[48] Chang SH, Wu CH, Tsai GJ. Effects of chitosan molecular weight on its antioxidant and antimutagenic properties. Carbohydr Polym 2018;181:1026–32.
[49] Li H, Xu Q, Chen Y, Wan A. Effect of concentration and molecular weight of chitosan and its derivative on the free radical scavenging ability. J Biomed Mater Res Part A 2014;102(3):911–16.
[50] Tomida H, Fujii T, Furutani N, Michihara A, Yasufuku T, Akasaki K, et al. Antioxidant properties of some different molecular weight chitosans. Carbohydr Res 2009;344(13):1690–6.

[51] Kim KW, Thomas RL. Antioxidative activity of chitosans with varying molecular weights. Food Chem 2007;101(1):308–13.
[52] Hu Z, Lu S, Cheng Y, Kong S, Li S, Li C, et al. Investigation of the Effects of Molecular Parameters on the Hemostatic Properties of Chitosan. Molecules 2018;23(12).
[53] Li J, Wu Y, Zhao L. Antibacterial activity and mechanism of chitosan with ultra high molecular weight. Carbohydr Polym 2016;148:200–5.
[54] Younes I, Sellimi S, Rinaudo M, Jellouli K, Nasri M. Influence of acetylation degree and molecular weight of homogeneous chitosans on antibacterial and antifungal activities. Int J Food Microbiol 2014;185:57–63.
[55] Park PJ, Je JY, Kim SK. Free radical scavenging activities of differently deacetylated chitosans using an ESR spectrometer. Carbohydr Polym 2004;55(1):17–22.
[56] Murthy SK. Nanoparticles in modern medicine: state of the art and future challenges. Int J Nanomedicine 2007;2(2):129–41.
[57] Mitchell MJ, Billingsley MM, Haley RM, Wechsler ME, Peppas NA, Langer R. Engineering precision nanoparticles for drug delivery. Nat Rev Drug Discov 2021;20(2):101–24.
[58] Barroso A, Mestre H, Ascenso A, Simões S, Reis C. Nanomaterials in wound healing: from material sciences to wound healing applications. Nano Select 2020;1(5):443–60.
[59] Mihai MM, Dima MB, Dima B, Holban AM. Nanomaterials for wound healing and infection control. Materials (Basel, Switzerland) 2019;12(13):2176.
[60] Pang C, Fan KS, Wei L, Kolar MK. Gene therapy in wound healing using nanotechnology. Wound Repair Regen 2021;29(2):225–39.
[61] Tiwari M, Jain P, Hariharpura RC, Udupa N, Rao JV. *In vitro* wound-healing effects of biosynthesized copper nanoparticles. Asian J Pharmaceut Sci 2016;11(1):158–9.
[62] Ahmad Raus R, Wan Nawawi WMF, Nasaruddin RR. Alginate and alginate composites for biomedical applications. Asian Journal of Pharmaceutical Sciences 2021;16(3):280–306.
[63] Okur ME, Karantas ID, Şenyiğit Z, Üstündağ Okur N, Siafaka PI. Recent trends on wound management: new therapeutic choices based on polymeric carriers. Asian J Pharmaceut Sci 2020;15(6):661–84.
[64] Mesa A, Mythatha GSS, Lodi RS, Ravuri S, Balli R. Chitosan nanoparticles: an overview on preparation, characterization and biomedical applications. In: Maddela NR, Chakraborty S, Prasad R, editors. Nanotechnology for advances in medical microbiology. Singapore: Springer Singapore; 2021. p. 393–427.
[65] Mohammed MA, Syeda JTM, Wasan KM, Wasan EK. An overview of chitosan nanoparticles and its application in non-parenteral drug delivery. Pharmaceutics 2017;9(4):53.
[66] Naskar S, Sharma S, Kuotsu K. Chitosan-based nanoparticles: an overview of biomedical applications and its preparation. J Drug Deliv Sci Technol 2019;49:66–81.
[67] Zielińska A, Carreiró F, Oliveira AM, Neves A, Pires B, Venkatesh DN, et al. Polymeric nanoparticles: production, characterization, toxicology and ecotoxicology. Molecules 2020;25(16):3731.
[68] Wang H, Qian J, Ding F. Recent advances in engineered chitosan-based nanogels for biomedical applications. Mater Chem B 2017;5(34):6986–7007.
[69] Kadam RN, Shendge RS, Pande VV. A review of nanotechnology with an emphasis on Nanoplex. Braz J Pharmaceut Sci 2015;51:255–63.
[70] Ghezzi M, Pescina S, Padula C, Santi P, Del Favero E, Cantù L, et al. Polymeric micelles in drug delivery: an insight of the techniques for their characterization and assessment in biorelevant conditions. J Control Rel 2021;332:312–36.
[71] Naskar A, Kim KS. Recent advances in nanomaterial-based wound-healing therapeutics. Pharmaceutics 2020;12(6):499.
[72] Naskar S, Kuotsu K, Sharma S. Chitosan-based nanoparticles as drug delivery systems: a review on two decades of research. J Drug Target 2019;27(4):379–93.
[73] Sahariah P, Másson M. Antimicrobial chitosan and chitosan derivatives: a review of the structure-activity relationship. Biomacromolecules 2017;18(11):3846–68.
[74] Tocco I, Zavan B, Bassetto F, Vindigni V. Nanotechnology-based therapies for skin wound regeneration. J Nanomater 2012;2012:714134.
[75] Wang T, Zheng Y, Shen Y, Shi Y, Li F, Su C, et al. Chitosan nanoparticles loaded hydrogels promote skin wound healing through the modulation of reactive oxygen species. Artif Cells Nanomed Biotechnol 2018;46(sup1):138–49.
[76] Pelegrino MT, Weller RB, Chen X, Bernardes JS, Seabra AB. Chitosan nanoparticles for nitric oxide delivery in human skin. Med Chem Comm 2017;8(4):713–9.
[77] Rajitha P, Gopinath D, Biswas R, Sabitha M, Jayakumar R. Chitosan nanoparticles in drug therapy of infectious and inflammatory diseases. Expert Opin Drug Deliv 2016;13(8):1177–94.
[78] Ta Q, Ting J, Harwood S, Browning N, Simm A, Ross K, et al. Chitosan nanoparticles for enhancing drugs and cosmetic components penetration through the skin. Eur J Pharm Sci 2021;160:105765.
[79] Cover NF, Lai-Yuen S, Parsons AK, Kumar A. Synergetic effects of doxycycline-loaded chitosan nanoparticles for improving drug delivery and efficacy. Int J Nanomedicine 2012;7:2411–9.
[80] Calvo P, Remuñán-López C, Vila-Jato JL, Alonso MJ. Novel hydrophilic chitosan-polyethylene oxide nanoparticles as protein carriers. J Appl Polym Sci 1997;63(1):125–32.
[81] Chen Y, Mohanraj VJ, Parkin JE. Chitosan-dextran Sulfate Nanoparticles for delivery of an anti-angiogenesis peptide. Lett Peptide Sci 2003;10(5):621–9.
[82] Denuziere A, Ferrier D, Damour O, Domard A. Chitosan–chondroitin sulfate and chitosan–hyaluronate polyelectrolyte complexes: biological properties. Biomaterials 1998;19(14):1275–85.
[83] Ichikawa S, Iwamoto S, Watanabe J. Formation of biocompatible nanoparticles by self-assembly of enzymatic hydrolysates of chitosan and carboxymethyl cellulose. Biosci Biotechnol Biochem 2005;69(9):1637–42.
[84] Jayakumar R, Chennazhi KP, Muzzarelli RAA, Tamura H, Nair SV, Selvamurugan N. Chitosan conjugated DNA nanoparticles in gene therapy. Carbohydr Polym 2010;79(1):1–8.
[85] Tan Q, Tang H, Hu J, Hu Y, Zhou X, Tao Y, et al. Controlled release of chitosan/heparin nanoparticle-delivered VEGF enhances regeneration of decellularized tissue-engineered scaffolds. Int J Nanomedicine 2011;6:929.
[86] Gaur U, Sahoo SK, De TK, Ghosh PC, Maitra A, Ghosh PK. Biodistribution of fluoresceinated dextran using novel nanoparticles evading reticuloendothelial system. Int J Pharm 2000;202(1):1–10.
[87] Maitra A, Ghosh PK, De TK, Sahoo SK. Process for the preparation of highly monodispersed polymeric hydrophilic nanoparticles. Google Patents 1999.
[88] Mitra S, Gaur U, Ghosh PC, Maitra AN. Tumour targeted delivery of encapsulated dextran–doxorubicin conjugate using chitosan nanoparticles as carrier. J Control Rel 2001;74(1):317–23.
[89] Bhattarai N, Ramay HR, Chou SH, Zhang M. Chitosan and lactic acid-grafted chitosan nanoparticles as carriers for prolonged drug delivery. Int J Nanomedicine 2006;1(2):181–7.
[90] Liu Y, Jia S, Wu Q, Ran J, Zhang W, Wu S. Studies of Fe_3O_4-chitosan nanoparticles prepared by co-precipitation

under the magnetic field for lipase immobilization. Catal Commun 2011;12(8):717–20.
[91] Thinh NN, Hanh PTB, Ha LTT, Anh LN, Hoang TV, Hoang VD, et al. Magnetic chitosan nanoparticles for removal of Cr(VI) from aqueous solution. Mater Sci Eng 2013;33(3):1214–8.
[92] Yuwei C, Jianlong W. Preparation and characterization of magnetic chitosan nanoparticles and its application for Cu(II) removal. Chem Eng J 2011;168(1):286–92.
[93] El-Shabouri MH. Positively charged nanoparticles for improving the oral bioavailability of cyclosporin-A. Int J Pharm 2002;249(1):101–8.
[94] Lin YH, Lin JH, Hong YS. Development of chitosan/poly-γ-glutamic acid/pluronic/curcumin nanoparticles in chitosan dressings for wound regeneration. J Biomed Mater Res Part B 2017;105(1):81–90.
[95] Riegger BR, Kowalski R, Hilfert L, Tovar GEM, Bach M. Chitosan nanoparticles via high-pressure homogenization-assisted miniemulsion crosslinking for mixed-matrix membrane adsorbers. Carbohydr Polym 2018;201:172–81.
[96] Brunel F, El Gueddari NE, Moerschbacher BM. Complexation of copper(II) with chitosan nanogels: toward control of microbial growth. Carbohydr Polym 2013;92(2):1348–56.
[97] Azadi A, Hamidi M, Rouini M-R. Methotrexate-loaded chitosan nanogels as 'Trojan Horses' for drug delivery to brain: preparation and *in vitro/in vivo* characterization. Int J Biol Macromol 2013;62:523–30.
[98] Chellappan DK, Yee NJ, Kaur Ambar Jeet Singh BJ, Panneerselvam J, Madheswaran T, Chellian J, et al. Formulation and characterization of glibenclamide and quercetin-loaded chitosan nanogels targeting skin permeation. Ther Deliv 2019;10(5):281–93.
[99] Arteche Pujana M, Pérez-Álvarez L, Cesteros Iturbe LC, Katime I. Biodegradable chitosan nanogels crosslinked with genipin. Carbohydr Polym 2013;94(2):836–42.
[100] Pérez-Álvarez L, Ruiz-Rubio L, Artetxe B, Vivanco Md, Gutiérrez-Zorrilla JM, Vilas-Vilela JL. Chitosan nanogels as nanocarriers of polyoxometalates for breast cancer therapies. Carbohydr Polym 2019;213:159–67.
[101] Nguyen MH, Yu H, Kiew TY, Hadinoto K. Cost-effective alternative to nano-encapsulation: amorphous curcumin–chitosan nanoparticle complex exhibiting high payload and supersaturation generation. Eur J Pharm Biopharm 2015;96:1–10.
[102] Nguyen MH, Lee SE, Tran TT, Bui CB, Nguyen THN, Vu NBD, et al. A simple strategy to enhance the *in vivo* wound-healing activity of curcumin in the form of self-assembled nanoparticle complex of curcumin and oligochitosan. Mater Sci Eng 2019;98:54–64.
[103] Yang Y, Wang S, Wang Y, Wang X, Wang Q, Chen M. Advances in self-assembled chitosan nanomaterials for drug delivery. Biotechnol Adv 2014;32(7):1301–16.
[104] Jones MC, Leroux JC. Polymeric micelles – a new generation of colloidal drug carriers. Eur J Pharm Biopharm 1999;48(2):101–11.
[105] Pham DT, Chokamonsirikun A, Phattaravorakarn V, Tiyaboonchai W. Polymeric micelles for pulmonary drug delivery: a comprehensive review. J Mater Sci 2021;56(3):2016–36.
[106] Monroe DM, Hoffman M. The clotting system – a major player in wound healing. Haemophilia 2012;18(s5):11–6.
[107] Biranje SS, Madiwale PV, Patankar KC, Chhabra R, Dandekar-Jain P, Adivarekar RV. Hemostasis and anti-necrotic activity of wound-healing dressing containing chitosan nanoparticles. Int J Biol Macromol 2019;121:936.
[108] Gopalakrishnan L, Ramana LN, Sethuraman S, Krishnan UM. Ellagic acid encapsulated chitosan nanoparticles as anti-hemorrhagic agent. Carbohydr Polym 2014;111:215–21.
[109] Lima JMd, Sarmento RR, Souza JRd, Brayner FA, Feitosa APS, Padilha R, et al. Evaluation of hemagglutination activity of chitosan nanoparticles using human erythrocytes. Biomed Res Int 2015;2015:247965.
[110] Wu Z, Zhou W, Deng W, Xu C, Cai Y, Wang X. Antibacterial and hemostatic thiol-modified chitosan-immobilized AgNPs composite sponges. ACS Appl Mater Interfaces 2020;12(18):20307–20.
[111] Yilmaz Atay H. Antibacterial Activity of Chitosan-Based Systems. Funct Chitosan 2020:457–89.
[112] Sami DG, Abdellatif A, Azzazy HME. Turmeric/oregano formulations for treatment of diabetic ulcer wounds. Drug Dev Ind Pharm 2020;46(10):1613–21.
[113] Jafari A, Hassanajili S, Karimi MB, Emami A, Ghaffari F, Azarpira N. Effect of organic/inorganic nanoparticles on performance of polyurethane nanocomposites for potential wound dressing applications. J Mech Behav Biomed Mater 2018;88:395–405.
[114] El-Kaliuoby MI, Amer M, Shehata N. Enhancement of nano-biopolymer Antibacterial activity by pulsed electric fields. Polymers (Basel) 2021;13(11).
[115] Tao Y, Qian LH, Xie J. Effect of chitosan on membrane permeability and cell morphology of Pseudomonas aeruginosa and Staphyloccocus aureus. Carbohydr Polym 2011;86(2):969–74.
[116] Ke CL, Deng FS, Chuang CY, Lin CH. Antimicrobial Actions and Applications of Chitosan. Polymers (Basel) 2021;13(6):904.
[117] Raafat D, von Bargen K, Haas A, Sahl H-G. Insights into the mode of action of chitosan as an antibacterial compound. Appl Environ Microbiol 2008;74(12):3764–73.
[118] Basha M, AbouSamra MM, Awad GA, Mansy SS. A potential antibacterial wound dressing of cefadroxil chitosan nanoparticles *in situ* gel: fabrication, *in vitro* optimization and *in vivo* evaluation. Int J Pharm 2018;544(1):129–40.
[119] Rozman NAS, Tong WY, Leong CR, Anuar MR, Karim S, Ong SK, et al. Homalomena pineodora essential oil nanoparticle inhibits diabetic wound pathogens. Sci Rep 2020;10(1):3307.
[120] Sun T, Zhan B, Zhang W, Qin D, Xia G, Zhang H, et al. Carboxymethyl chitosan nanoparticles loaded with bioactive peptide OH-CATH30 benefit nonscar wound healing. Int J Nanomedicine 2018;13:5771–86.
[121] Zou P, Lee WH, Gao Z, Qin D, Wang Y, Liu J, et al. Wound dressing from polyvinyl alcohol/chitosan electrospun fiber membrane loaded with OH-CATH30 nanoparticles. Carbohydr Polym 2020;232:115786.
[122] Wang K, Pan S, Qi Z, Xia P, Xu H, Kong W, et al. Recent advances in chitosan-based metal nanocomposites for wound healing applications. Adv Mater Sci Eng 2020;2020:3827912.
[123] Li C, Fu R, Yu C, Li Z, Guan H, Hu D, et al. Silver nanoparticle/chitosan oligosaccharide/poly(vinyl alcohol) nanofibers as wound dressings: a preclinical study. Int J Nanomedicine 2013;8:4131–45.
[124] Pansara C, Mishra R, Mehta T, Parikh A, Garg S. Formulation of chitosan stabilized silver nanoparticle-containing wound healing film: *in vitro* and *in vivo* characterization. J Pharm Sci 2020;109(7):2196–205.
[125] Dhanalakshmi V, Nimal TR, Sabitha M, Biswas R, Jayakumar R. Skin and muscle permeating antibacterial nanoparticles for treating Staphylococcus aureus infected wounds. J Biomed Mater Res Part B 2016;104(4):797–807.
[126] El-Feky GS, Sharaf SS, El Shafei A, Hegazy AA. Using chitosan nanoparticles as drug carriers for the

development of a silver sulfadiazine wound dressing. Carbohydr Polym 2017;158:11–9.
[127] Shahzad A, Khan A, Afzal Z, Umer MF, Khan J, Khan GM. Formulation development and characterization of cefazolin nanoparticles-loaded cross-linked films of sodium alginate and pectin as wound dressings. Int J Biol Macromol 2019;124:255–69.
[128] Basit HM, Mohd Amin MC, Ng S-F, Katas H, Shah SU, Khan NR. Formulation and evaluation of microwave-modified chitosan-curcumin nanoparticles—A promising nanomaterials platform for skin tissue regeneration applications following burn wounds. Polymers (Basel) 2020;12(11).
[129] Lin YH, Lin JH, Li TS, Wang SH, Yao CH, Chung WY, et al. Dressing with epigallocatechin gallate nanoparticles for wound regeneration. Wound Repair Regen 2016;24(2):287–301.
[130] Ehterami A, Salehi M, Farzamfar S, Vaez A, Samadian H, Sahrapeyma H, et al. *In vitro* and *in vivo* study of PCL/COLL wound dressing loaded with insulin-chitosan nanoparticles on cutaneous wound healing in rats model. Int J Biol Macromol 2018;117:601–9.
[131] Díez-Pascual AM, Díez-Vicente AL. Wound healing bionanocomposites based on castor oil polymeric films reinforced with chitosan-modified ZnO nanoparticles. Biomacromolecules 2015;16(9):2631–44.
[132] Ding L, Shan X, Zhao X, Zha H, Chen X, Wang J, et al. Spongy bilayer dressing composed of chitosan–Ag nanoparticles and chitosan–Bletilla striata polysaccharide for wound healing applications. Carbohydr Polym 2017;157:1538–47.
[133] Dorazilová J, Muchová J, Šmerková K, Kočiová S, Diviš P, Kopel P, et al. Synergistic Effect of Chitosan and Selenium Nanoparticles on Biodegradation and Antibacterial Properties of Collagenous Scaffolds Designed for Infected Burn Wounds. Nanomaterials 2020;10(10).
[134] Hajji S, Khedir SB, Hamza-Mnif I, Hamdi M, Jedidi I, Kallel R, et al. Biomedical potential of chitosan-silver nanoparticles with special reference to antioxidant, antibacterial, hemolytic and *in vivo* cutaneous wound healing effects. Biochimica et Biophysica Acta (BBA) - General Subjects 2019;1863(1):241–54.
[135] Lu B, Ye H, Shang S, Xiong Q, Yu K, Li Q, et al. Novel wound dressing with chitosan gold nanoparticles capped with a small molecule for effective treatment of multiantibiotic-resistant bacterial infections. Nanotechnology 2018;29(42):425603.
[136] Parthasarathy A, Vijayakumar S, Malaikozhundan B, Thangaraj MP, Ekambaram P, Murugan T, et al. Chitosan-coated silver nanoparticles promoted antibacterial, antibiofilm, wound-healing of murine macrophages and antiproliferation of human breast cancer MCF 7 cells. Polym Test 2020;90:106675.
[137] Peng Y, Song C, Yang C, Guo Q, Yao M. Low molecular weight chitosan-coated silver nanoparticles are effective for the treatment of MRSA-infected wounds. Int J Nanomedicine 2017;12:295–304.
[138] Shah A, Ali Buabeid M, Arafa E-SA, Hussain I, Li L, Murtaza G. The wound healing and antibacterial potential of triple-component nanocomposite (chitosan-silver-sericin) films loaded with moxifloxacin. Int J Pharm 2019;564:22–38.
[139] Verma J, Kanoujia J, Parashar P, Tripathi CB, Saraf SA. Wound healing applications of sericin/chitosan-capped silver nanoparticles incorporated hydrogel. Drug Deliv Transl Res 2017;7(1):77–88.
[140] Vijayakumar S, Malaikozhundan B, Parthasarathy A, Saravanakumar K, Wang M-H, Vaseeharan B. Nano biomedical potential of biopolymer chitosan-capped silver nanoparticles with special reference to antibacterial, antibiofilm, anticoagulant and wound dressing material. J Cluster Sci 2020;31(2):355–66.
[141] Oryan A, Alemzadeh E, Tashkhourian J, Nami Ana SF. Topical delivery of chitosan-capped silver nanoparticles speeds up healing in burn wounds: a preclinical study. Carbohydr Polym 2018;200:82–92.
[142] Muraina I, Suleiman MM, Eloff J. Can MTT be used to quantify the antioxidant activity of plant extracts? Phytomedicine 2009;16:665–8.
[143] Kaparekar PS, Pathmanapan S, Anandasadagopan SK. Polymeric scaffold of gallic acid loaded chitosan nanoparticles infused with collagen-fibrin for wound dressing application. Int J Biol Macromol 2020;165:930–47.
[144] Hu Q, Wang T, Zhou M, Xue J, Luo Y. *In vitro* antioxidant-activity evaluation of gallic-acid-grafted chitosan conjugate synthesized by free-radical-induced grafting method. J Agric Food Chem 2016;64(29):5893–900.
[145] Samadarsi R, Dutta D. Anti-oxidative effect of mangiferin-chitosan nanoparticles on oxidative stress-induced renal cells. Int J Biol Macromol 2020;151:36–46.
[146] Kumar SP, Birundha K, Kaveri K, Devi KTR. Antioxidant studies of chitosan nanoparticles containing naringenin and their cytotoxicity effects in lung cancer cells. Int J Biol Macromol 2015;78:87–95.
[147] Friedman AJ, Phan J, Schairer DO, Champer J, Qin M, Pirouz A, et al. Antimicrobial and anti-inflammatory activity of chitosan-alginate nanoparticles: a targeted therapy for cutaneous pathogens. J Invest Dermatol 2013;133(5):1231–9.
[148] Li F, Shi Y, Liang J, Zhao L. Curcumin-loaded chitosan nanoparticles promote diabetic wound healing via attenuating inflammation in a diabetic rat model. J Biomater Appl 2019;34(4):476–86.
[149] Hou B, Qi M, Sun J, Ai M, Ma X, Cai W, et al. Preparation, characterization and wound healing effect of vaccarin-chitosan nanoparticles. Int J Biol Macromol 2020;165:3169–79.
[150] Choudhary A, Kant V, Jangir BL, Joshi VG. Quercetin loaded chitosan tripolyphosphate nanoparticles accelerated cutaneous wound healing in Wistar rats. Eur J Pharmacol 2020;880:173172.
[151] Honnegowda TM, Kumar P, Udupa EGP, Kumar S, Kumar U, Rao P. Role of angiogenesis and angiogenic factors in acute and chronic wound healing. Plastic Aesthetic Res 2015;2:243–9.
[152] Tonnesen MG, Feng X, Clark RA. Angiogenesis in wound healing. J Investig Dermatol Symp Proc 2000;5(1):40–6.
[153] DiPietro LA. Angiogenesis and wound repair: when enough is enough. J Leukoc Biol 2016;100(5):979–84.
[154] Chi J, Zhang X, Chen C, Shao C, Zhao Y, Wang Y. Antibacterial and angiogenic chitosan microneedle array patch for promoting wound healing. Bioactive Mater 2020;5(2):253–9.
[155] Yar M, Shahzad S, Shahzadi L, Shahzad SA, Mahmood N, Chaudhry AA, et al. Heparin binding chitosan derivatives for production of pro-angiogenic hydrogels for promoting tissue healing. Mater. Sci. Eng.: C 2017;74:347–56.
[156] Zahiri M, Khanmohammadi M, Goodarzi A, Ababzadeh S, Sagharjoghi Farahani M, Mohandesnezhad S, et al. Encapsulation of curcumin loaded chitosan nanoparticle within poly (ε-caprolactone) and gelatin fiber mat for wound healing and layered dermal reconstitution. Int J Biol Macromol 2020;153:1241–50.
[157] Kant V, Jangir BL, Kumar V, Nigam A, Sharma V. Quercetin accelerated cutaneous wound healing in rats by modulation of different cytokines and growth factors. Growth Factors 2020;38(2):105–19.

[158] Guo X, Xu D, Zhao Y, Gao H, Shi X, Cai J, et al. Electroassembly of chitin nanoparticles to construct freestanding hydrogels and high porous aerogels for wound healing. ACS Appl Mater Interfaces 2019;11(38):34766–76.
[159] Li C-w, Wang Q, Li J, Hu M, Shi S-j, Li Z-w, et al. Silver nanoparticles/chitosan oligosaccharide/poly(vinyl alcohol) nanofiber promotes wound healing by activating TGFβ1/Smad signaling pathway. Int J Nanomedicine 2016;11:373–86.
[160] Sinno H, Prakash S. Complements and the wound healing cascade: an updated review. Plast Surg Int 2013;2013:146764.
[161] Xue M, Jackson CJ. Extracellular matrix reorganization during wound healing and its iImpact on abnormal scarring. Adv Wound Care 2015;4(3):119–36.
[162] Corr DT, Hart DA. Biomechanics of scar tissue and uninjured skin. Adv Wound Care 2013;2(2):37–43.
[163] Ricard-Blum S. The collagen family. Cold Spring Harb Perspect Biol 2011;3(1) a004978.
[164] Colgrave ML, Allingham PG, Jones A. Hydroxyproline quantification for the estimation of collagen in tissue using multiple reaction monitoring mass spectrometry. J Chromatogr A 2008;1212(1):150–3.
[165] Ignat'eva NY, Danilov NA, Averkiev SV, Obrezkova MV, Lunin VV, Sobol' EN. Determination of hydroxyproline in tissues and the evaluation of the collagen content of the tissues. J Anal Chem 2007;62(1):51–7.
[166] Lopes Rocha Correa V, Assis Martins J, Ribeiro de Souza T, de Castro Nunes Rincon G, Pacheco Miguel M, Borges de Menezes L, et al. Melatonin loaded lecithin-chitosan nanoparticles improved the wound healing in diabetic rats. Int J Biol Macromol 2020;162:1465–75.
[167] Zi-Wei L, Li CW, Wang Q, Shi SJ, Hu M, Zhang Q, et al. The cellular and molecular mechanisms underlying silver nanoparticle/chitosan oligosaccharide/poly(vinyl alcohol) nanofiber-mediated wound healing. J Biomed Nanotechnol 2017;13(1):17–34.
[168] Blažević F, Milekić T, Romić MD, Juretić M, Pepić I, Filipović-Grčić J, et al. Nanoparticle-mediated interplay of chitosan and melatonin for improved wound epithelialisation. Carbohydr Polym 2016;146:445–54.
[169] Zhang P, Liu C. Enhancement of skin wound healing by rhEGF-loaded carboxymethyl chitosan nanoparticles. Polymers (Basel) 2020;12(7).
[170] Sun M, Xie Q, Cai X, Liu Z, Wang Y, Dong X, et al. Preparation and characterization of epigallocatechin gallate, ascorbic acid, gelatin, chitosan nanoparticles and their beneficial effect on wound healing of diabetic mice. Int J Biol Macromol 2020;148:777–84.
[171] El-Feky GS, El-Banna ST, El-Bahy GS, Abdelrazek EM, Kamal M. Alginate coated chitosan nanogel for the controlled topical delivery of Silver sulfadiazine. Carbohydr Polym 2017;177:194–202.
[172] Negi P, Sharma G, Verma C, Garg P, Rathore C, Kulshrestha S, et al. Novel thymoquinone loaded chitosan-lecithin micelles for effective wound healing: development, characterization, and preclinical evaluation. Carbohydr Polym 2020;230:115659.
[173] Karri VVSR, Kuppusamy G, Talluri SV, Mannemala SS, Kollipara R, Wadhwani AD, et al. Curcumin loaded chitosan nanoparticles impregnated into collagen-alginate scaffolds for diabetic wound healing. Int J Biol Macromol 2016;93:1519–29.
[174] Shende P, Gupta H. Formulation and comparative characterization of nanoparticles of curcumin using natural, synthetic and semi-synthetic polymers for wound healing. Life Sci 2020;253:117588.
[175] Karimi Dehkordi N, Minaiyan M, Talebi A, Akbari V, Taheri A. Nanocrystalline cellulose-hyaluronic acid composite enriched with GM-CSF loaded chitosan nanoparticles for enhanced wound healing. Biomed Mater 2019;14(3):035003.
[176] Ribeiro MC, Correa VLR, Silva FKLd, Casas AA, Chagas AdLd, Oliveira LPd, et al. Wound healing treatment using insulin within polymeric nanoparticles in the diabetes animal model. Eur J Pharm Sci 2020;150:105330.
[177] Tanha S, Rafiee-Tehrani M, Abdollahi M, Vakilian S, Esmaili Z, Naraghi ZS, et al. G-CSF loaded nanofiber/nanoparticle composite coated with collagen promotes wound healing *in vivo*. J Biomed Mater Res Part A 2017;105(10):2830–42.
[178] Lei W, Yu C, Lin H, Zhou X. Development of tacrolimus-loaded transfersomes for deeper skin penetration enhancement and therapeutic effect improvement *in vivo*. Asian Journal of Pharmaceutical Sciences 2013;8(6):336–45.
[179] Du J, Wong KKY. 9 - Nanomaterials for wound healing: scope and advances. In: Cui W, Zhao X, editors. Micro and nano technologies, theranostic bionanomaterials. Elsevier; 2019. p. 211–30.
[180] Xu C, Akakuru OU, Ma X, Zheng J, Zheng J, Wu A. Nanoparticle-based wound dressing: recent progress in the detection and therapy of bacterial infections. Bioconjug Chem 2020;31(7):1708–23.
[181] Bilal M, Zhao Y, Rasheed T, Ahmed I, Hassan STS, Nawaz MZ, et al. Biogenic nanoparticle–chitosan conjugates with antimicrobial, antibiofilm, and anticancer potentialities: development and characterization. Int J Environ Res Public Health 2019;16(4):598.
[182] Khan F, Pham DTN, Oloketuyi SF, Manivasagan P, Oh J, Kim YM. Chitosan and their derivatives: antibiofilm drugs against pathogenic bacteria. Colloids Surf B 2020;185:110627.
[183] Rivera Aguayo P, Bruna Larenas T, Alarcón Godoy C, Cayupe Rivas B, González-Casanova J, Rojas-Gómez D, et al. Antimicrobial and antibiofilm capacity of chitosan nanoparticles against wild type strain of pseudomonas sp. isolated from milk of cows diagnosed with bovine mastitis. Antibiotics (Basel) 2020;9(9).
[184] Campani V, Pagnozzi E, Mataro I, Mayol L, Perna A, D'Urso F, et al. Chitosan gel to treat pressure ulcers: a clinical pilot study. Pharmaceutics 2018;10(1):15.
[185] Mo X, Cen J, Gibson E, Wang R, Percival SL. An open multicenter comparative randomized clinical study on chitosan. Wound Repair Regen 2015;23(4):518–24.
[186] Bellich B, D'Agostino I, Semeraro S, Gamini A, Cesàro A. The good, the bad and the ugly" of chitosans. Mar Drugs 2016;14(5):99.
[187] Szymańska E, Winnicka K. Stability of chitosan—A challenge for pharmaceutical and biomedical applications. Mar Drugs 2015;13(4).
[188] Islam N, Dmour I, Taha MO. Degradability of chitosan micro/nanoparticles for pulmonary drug delivery. Heliyon 2019;5(5):e01684.
[189] Nowack B, Bucheli TD. Occurrence, behavior and effects of nanoparticles in the environment. Environ Pollut 2007;150(1):5–22.
[190] Huang YW, Cambre M, Lee HJ. The toxicity of nanoparticles depends on multiple molecular and physicochemical mechanisms. Int J Mol Sci 2017;18(12).
[191] Vauthier C, Bouchemal K. Methods for the preparation and manufacture of polymeric nanoparticles. Pharm Res 2009;26(5):1025–58.